

EXPRESSION OF FOLLICLE STIMULATING HORMONE RECEPTOR VARIANTS
DURING THE SHEEP ESTROUS CYCLE

by

RACHAEL R. SULLIVAN

B.S., Kansas State University, 2001

A THESIS

submitted in partial fulfillment of the requirements for the degree

MASTER OF SCIENCE

Department of Animal Sciences and Industry
College of Agriculture

KANSAS STATE UNIVERSITY
Manhattan, Kansas

2009

Approved by:

Major Professor
Timothy G. Rozell

Abstract

Several alternatively-spliced mRNA transcripts of the follicle stimulating hormone receptor (*FSHR*) have been identified in sheep, including FSHR-1 (G protein-coupled form), FSHR-2 (dominant negative form), and FSHR-3 (growth factor type-1 form). Coupling of the *FSHR* to signaling pathways which activate different downstream effectors leads to speculation that specific splice variants may be transcribed under differing physiological conditions.

This is the first study to correlate expression patterns of FSHR-1, FSHR-2, and FSHR-3 and development of follicles in the mature sheep ovary. In Experiment 1, 8 Suffolk-cross ewes were allowed to come into estrus naturally and were euthanized 24 (n=3), 36 (n=3), and 48 (n=2) hours after the onset of estrus. In Experiment 2, 7 Suffolk-cross ewes received CIDRs for 14 days. At CIDR removal, PMSG (500IU) was administered to treatment ewes (n=3), while controls (n=4) received no PMSG. Ewes were euthanized 24 (n=4; 2 CIDR only, 2 PMSG) or 36 (n=3; 2 CIDR only, 1 PMSG) hours later. All visible follicles were aspirated and pooled according to follicular diameter: small (≤ 2.0 mm), medium (2.1-4.0 mm), large (4.1-6.0 mm), and preovulatory (≥ 6.1 mm). Granulosa cells were separated from follicular fluid by centrifugation. Total RNA was extracted from granulosa cells (GC) and reversed transcribed. The resulting cDNA was subjected to qPCR, using primer sets designed to amplify each variant specifically.

For Experiment 1, regardless of time after onset of estrus, relative expression of FSHR-3 exceeded that of both FSHR-1 and FSHR-2 in medium follicles ($p < 0.01$), and tended to be higher in small follicles ($p=0.09$). For Experiment 2, treatment with PMSG did not significantly

alter expression patterns of *FSHR* variants ($p=0.18$). The FSHR-3 was expressed higher than FSHR-2 in all follicle sizes ($p < 0.01$) and was numerically more highly expressed than FSHR-1, although this difference was not significant ($p > 0.11$).

These experiments show that in addition to the well characterized G protein-coupled form of the *FSHR*, alternatively spliced variants of the *FSHR* may participate in follicular dynamics during the first follicular wave of the sheep estrous cycle. Furthermore, these results would indicate that an “alternatively” spliced form of the *FSHR* (FSHR-3) is the predominant form of the *FSHR* in the sheep.

Table of Contents

List of Figures	vi
List of Tables	viii
Acknowledgements	ix
CHAPTER 1 - LITERATURE REVIEW	1
Introduction	1
Follicular Development	2
Waves of Follicular Growth	5
Gonadotropins	7
Gonadotropin Receptors	9
Follicle Stimulating Hormone Receptor Gene	9
Follicle Stimulating Hormone Receptor Structure	10
G Proteins	11
Cessation of signaling	12
Gene Splicing	12
FSHR Alternative Splice Variants	13
Seasonality	15
CHAPTER 2 - EXPRESSION OF FOLLICLE STIMULATING HORMONE RECEPTOR VARIANTS DURING THE ESTROUS CYCLE OF SHEEP	18
Introduction	18
Materials and Methods	20
Animals and Sample Collection	20
RNA Isolation and DNase Treatment	22
Reverse Transcription – Polymerase Chain Reaction	22
Real-Time Polymerase Chain Reaction	23
RIA	27
Statistical Analysis	27
Analysis of Techniques	28
RNA Quantitation	28

RNA Quality	30
Agarose Gel Electrophoresis.....	32
Melting Curve Analysis	32
Results.....	34
Discussion.....	47
CHAPTER 3 - References	52
Appendix A - Protocols and Forms	59
Aspiration Protocol.....	59
RNA Extraction from Trizol samples.....	60
DNase Treat RNA TURBO DNA- <i>free</i> Protocol	62
RT-PCR Protocol - SuperScript III First-Strand Synthesis SuperMix	63
Real-Time PCR Protocol - Platinum SYBR Green qPCR SuperMix-UDG with ROX.....	64
DNA Gel Protocol	65
Estradiol RIA Protocol.....	66
Progesterone RIA Protocol	70
RNA Quality Protocol-Agilent 2100 Bioanalyzer with Agilent 6000 Nano Kit.....	71
Appendix B - Reagents and Supplies.....	73

List of Figures

Figure 2.1. Nucleotide sequence and exon structure for FSHR-3.	24
Figure 2.2. Nucleotide sequence and exon structure for FSHR-2.	25
Figure 2.3. Nucleotide sequence and exon structure for FSHR-1.	26
Figure 2.4. Comparison of quantitation methods after extraction of total RNA—Experiment 1.	29
Figure 2.5. Comparison of quantitation methods after extraction of total RNA—Experiment 2.	30
Figure 2.6. Quality assessment of total RNA from sheep granulosa cells.....	31
Figure 2.7. Representative melt-curve analysis of primer sets and amplicon size.	33
Figure 2.8. Expression of gonadotropin receptors within different sized sheep follicles— Experiment 1.	35
Figure 2.9. Expression of gonadotropin receptors across different sized sheep follicles— Experiment 1.	36
Figure 2.10. Expression of gonadotropin receptors within different sized sheep follicles— Experiment 2.	37
Figure 2.11. Expression of gonadotropin receptors across different sized sheep follicles— Experiment 2.	38
Figure 2.12. Expression of gonadotropin receptors at 24 hours after CIDR removal within small and medium sheep follicles—Experiment 2.	39
Figure 2.13. Expression of gonadotropin receptors at 36 hours after CIDR removal within small and medium sheep follicles—Experiment 2.	40
Figure 2.14. Expression of gonadotropin receptors within large sheep follicles—Experiment 2.	41
Figure 2.15. Estradiol and progesterone concentrations in follicular fluid from different-sized sheep follicles—Experiment 1.	42
Figure 2.16. Correlation between estradiol to progesterone ratio and gene expression in small and medium sheep follicles—Experiment 1.	43
Figure 2.17. Estradiol and progesterone concentrations in follicular fluid from different-sized sheep follicles—Experiment 2.	44

Figure 2.18. Correlation between estradiol to progesterone ratio and gene expression in small and medium sheep follicles—Experiment 2. 45

List of Tables

Table 2.1. Description of primers used for quantitative real-time PCR.	23
Table 2.2. Average values for sample collection parameters in Experiment 1 and 2.....	47

Acknowledgements

I wish to acknowledge the plethora of people that helped me in order that I might graduate. I will start by thanking my mom for bugging me about going back to graduate school. Even though it annoyed me tremendously at the time, I am grateful that I eventually heeded her advice (right again, Mom). I want to thank Dr. Timothy Rozell for going out on a limb and agreeing to be my major professor, especially considering he knew my track record as an undergraduate. Thankfully, I was much more studious in graduate school.

I never could have completed my lab work without the aid of Dr. David Grieger, and Dr. Douglas Eborn, who were there for the “good times” as I looked for the infamous “R3” (which I looked for just about everywhere: in cows, pigs, two cell culture lines, under my lab notebook...and eventually in sheep). Thank you both for your patience and understanding as I learned new lab techniques, and for help interpreting results. I also wanted to thank Dr. Grieger for teaching me how to rectally palpate cattle (an awkward thing to acknowledge, but true nonetheless). Colleen Hill’s assistance in running radioimmunoassays is also appreciated.

Several people helped coordinate animal care and tissue sampling, and I wish to acknowledge them: Dr. Tim Rozell, for helping collect samples and load ewes in the wee hours of the morning; Dr. Brian Faris, for helping at the Sheep Unit (although his pregnancy detection skills did leave a little to be desired), and for letting me drive that beautiful truck and trailer rig around town; Dr. Jeffrey Stevenson for setting up the HeatWatch[®] heat detection system; Chris Bauerle, for animal care and sampling assistance; and Douglas Eborn and Carlie Spiker for sheep wrangling and sampling assistance. To date, Douglas is the only adult I’ve seen ride a sheep; his back has never been the same (that mutton busting is tougher than it looks). There were also several folks at the KSU Diagnostic Lab who helped with euthanasia and tissue collection including: Dr. Brad DeBey, Dr. Jerome Nietfeld, Dr. Matt Miesner, and Tracy Weston.

Finally, I’d like to thank my husband, Matt, for his daily patience and support as I fumbled my way through graduate school. I am thankful for the sacrifices he made in order that I might complete my degree.

CHAPTER 1 - LITERATURE REVIEW

Introduction

Follicular development begins before birth in some species, including the sheep. The sheep fetus begins follicular growth approximately 100 days into gestation, or 50 days before birth [1]. By day 135 of gestation, the first antral follicle appears [2]. At birth, germ cell division is complete, and each follicle contains an arrested primary oocyte that progresses no further than the diplotene stage of meiosis I. Oocyte growth remains arrested until a follicle undergoes recruitment, selection, and is exposed to the preovulatory LH surge.

The process of follicular development is dependent upon endocrine support which is provided by gonadotropin hormones, including follicle stimulating hormone (FSH) and luteinizing hormone (LH). Follicle stimulating hormone has been shown to have many functions during follicular growth [3]. It is intriguing that one hormone could promote different responses from follicles growing under similar conditions. One possibility for different modes of action from the same hormone may be due to the receptor to which it binds [4].

The follicle stimulating hormone receptor (FSHR) is a large glycoprotein hormone receptor, located within ovarian follicles on granulosa cells. In 1993, the ovine G protein coupled form of the *FSHR* (FSHR-1) was cloned and sequenced [5], based on DNA sequences previously described for the rat [6]. At that time, several alternatively spliced variants of the ovine *FSHR* were found [5, 7]. In-vitro studies determined that two variants, FSHR-2 and FSHR-3, would likely have functional significance [8, 9]. FSHR-2 is thought to act as a dominant-negative receptor and prevent downstream signaling [8]. FSHR-3 is thought to act as a growth factor type I receptor and stimulate proliferative pathways [9]. These alternative

signaling pathways may help to explain the diverse actions of FSH during follicular development.

Since the first in-vitro studies, little research has been conducted to examine the in vivo expression of *FSHR* variants. In order to gain a clearer picture of the actions of both FSH and *FSHR* variants during follicular development, it is necessary to look at the pattern of expression of *FSHR* variants at different times during the estrous cycle. If variants are differentially expressed, further studies may be needed to determine the functions of the newly discovered variants.

Follicular Development

At any given time after the first follicles are formed, follicles of most developmental stages can be found within the ovary. The least developed follicle type is the primordial follicle. Resting primordial follicles have a single layer of flattened granulosa cells surrounding an ovoid or spherical oocyte [10]. The majority of a follicle's life is spent in the resting primordial pool. It is not completely clear what mechanisms cause some resting primordial follicles to become activated, and join the group of growing follicles. When cortical pieces of ovary with large numbers of primordial follicles are grown in culture, the vast majority of primordial follicles spontaneously activate and start growing [11]. This is in sharp contrast to the natural slow progression of follicles out of the resting pool. This suggests that in vivo, inhibitory factors (from cells distinct from those found within follicles) keep the number of activating primordial follicles in check [12].

Once resting primordial follicles are activated, they begin to express markers of cell proliferation, such as proliferating cell nuclear antigen (PCNA) [11]. The layer of flattened

granulosa cells begin to change shape and become cuboidal as they transition to primary follicles [10]. Some primary follicles express FSH receptors [13]; however, it is unclear to what extent they are able to respond to FSH. Two growth factors have been demonstrated to be essential for primary to secondary follicle transition in sheep [14]: Growth and Differentiation Factor 9 (GDF9) and Bone Morphogenetic Protein 15 (BMP15) [15-17]. Sheep that are immunized against either GDF9 or BMP15 fail to have follicular growth beyond the primary stage [15, 18]. There are also five naturally occurring point mutations in *BMP15* in breeds such as the Cambridge and Belclare [17]. Each mutation causes the same phenotype. Ewes heterozygous for the *BMP15* mutation have increased fertility; yet ewes homozygous for the *BMP15* mutation have arrested follicular development at the primary stage [14, 17, 19]. This affirms that BMP15 exerts negative inhibition on follicular development. Removal of a single copy of the gene allows more follicles to remain viable. However, when both copies of the gene are affected, follicular development ceases, as *BMP15* is needed for primary to secondary follicle transition [15, 17].

A natural point mutation in *GDF9* also exists [16]. As with the *BMP15* mutation, ewes homozygous for the *GDF9* mutation are infertile, but heterozygotes have increased fertility. At least one functioning copy of *GDF9* and *BMP15* are needed for primary to secondary follicle transition.

Secondary follicles have two layers of cuboidal granulosa cells and also have a theca interna layer on the outer boundary of the basement membrane [2]. Because many enzymes needed for steroidogenesis are not yet expressed by theca cells, it is thought that they are not steroidogenically active until the large preantral stage [20]. In sheep, all secondary follicles were shown to express *FSHR* mRNA in granulosa cells [13]. Even though the receptor is present, it is

accepted that follicle development to the antral (< 0.23 mm) stage is not completely dependent upon gonadotropins, but is gonadotropin responsive [21].

Tertiary follicles have more than two layers of cuboidal granulosa cells, and the formation of a small antrum, or fluid-filled cavity. Before antrum formation, follicle growth is slow, taking about 130 days between activation to antrum formation. After antrum formation, follicles grow more quickly, as it only takes about 45 days from antrum formation to reach preovulatory size [22]. Formation of the antrum pushes the oocyte to one side of the follicle. Some granulosa cells remain in contact with the oocyte (cumulus GC), while others form layers on the inside of the basement membrane (mural GC). Once sheep follicles reach 2 mm in diameter, they are considered to be gonadotropin dependent. After reaching that diameter, if follicles do not receive adequate gonadotropin support, they will undergo atresia. This was illustrated in sheep by Dufour et al. (1979), when only 4 days post hypophysectomy all “large” antral follicles began to undergo atresia [23]. If antral follicles receive adequate gonadotropin support, they will continue to grow.

One important function of antral follicles is to begin producing the steroid hormones, estrogen and progesterone. Theca interna cells have enzymes which convert pregnenolone to androstenedione. Granulosa cells have enzymes which convert androgens to estrogens [24]. Free cholesterol is shuttled to the mitochondria of the cell, where it undergoes side chain cleavage by the enzyme C27 side-chain cleavage P450. This renders the compound pregnenolone which is transported to the smooth endoplasmic reticulum. Pregnenolone can then enter one of two pathways: the 5-ene-3 β -hydroxy (5-ene) pathway or the 4-en-3-oxo (4-en) pathway. Pregnenolone must enter the 4-en pathway to be converted to progesterone. There are many intermediate compounds that can be formed depending on the enzyme repertoire of the cell, and

the order in which enzymes are encountered. Estradiol can be formed after several intermediates are converted to testosterone or estrone. Testosterone is converted to estradiol by aromatase P450. After synthesis, steroids can enter the bloodstream and act in an endocrine manner. Steroids contribute to follicular growth through both positive and negative feedback mechanisms.

In sheep, often more than one follicle per estrous cycle escapes atresia, grows to the preovulatory (or Graafian) follicle size and ultimately ovulates. Follicular growth from 2 mm to preovulatory size (≥ 6 mm) is very rapid, occurs within a day or two after the corpus luteum begins to regress. In order for a follicle to escape atresia, it must acquire LH receptors in the GC layer. It is unclear what mechanisms allow transcription of LH receptor in the granulosa cell layer in the future “dominant” follicles, while other “subordinate” follicles do not acquire LH receptor.

Waves of Follicular Growth

In sheep, there has been considerable controversy about whether or not follicular development occurs in waves. Follicular waves were originally defined in cattle by Rajakoski (1960), as the changes in the number of follicles among the days of the estrous cycle [25]. Rajakoski developed this definition based upon the patterns of follicular growth he observed from ovaries of cattle he obtained at slaughter. He noted that more follicles were present on certain days of the estrous cycle, and postulated that two “waves” of follicular development occur in the cow. The use of ultrasonography allowed Rajakoski’s hypothesis to be proven in cattle by Pierson and Ginther (1988) [26]. In cattle, it is now widely accepted that follicular growth occurs in waves [27].

Follicular waves in sheep were noted as early as 1971 [28], with various studies agreeing [29] or disagreeing [30] with the notion of waves in sheep. Evans et al. (2002) published evidence in favor of follicular development in waves during the estrous cycle of sheep [31]. These investigators wanted to statistically characterize the number and size of follicles present on each day of the cycle, as lack of statistical proof had been one of the main arguments against follicular waves in sheep [32]. Monoovulatory species of sheep were monitored via ultrasonography throughout one or two estrous cycles and two to four waves of follicular development were seen. Considering that the sheep estrous cycle is relatively short, ewes with more than two follicular waves undergo rapid follicular turnover. It is suspected that earlier studies which were unable to detect waves of follicular growth [30] may be because the turnover rate was too great [31].

Although waves of follicular growth are generally characterized by monitoring antral follicle development via ultrasonography, the process begins with activation of primordial follicles. In sheep, it is estimated that 2-3 follicles are activated from the primordial pool each day [33]. It takes about 180 days for one of those follicles to reach an ovulatory diameter [22]. Once these follicles reach 2 mm in diameter, they are considered gonadotropin responsive. It is from this pool of follicles that a growing cohort emerges [31]. Factors that contribute to emergence are largely unknown, but it occurs during a transient rise in circulating FSH concentrations [34, 35]. Once this cohort is recruited, there is a common growth phase in which no follicles exert dominance over the others, followed by the process of selection. Several intrafollicular factors are thought to play a role in selection, including IGF-1 and its binding proteins [36]. After selection, one or two follicles will gain LHR in the granulosa cell layer. As circulating FSH declines, these follicles are then able to respond to LH to meet their

gonadotropin requirement. Selection is accompanied by diameter deviation, in which the follicles that have become LH dependent grow at a faster rate than follicles which still require FSH for growth [31].

Although follicular waves occur during the luteal and follicular phases of the estrous cycle, the dominant follicles will only ovulate if no functioning corpora lutea are present. If functional CL are present, the dominant follicles will regress. If no CL is present, dominant follicles will continue to grow and secrete more estradiol. As higher concentrations of estradiol enter circulation, they exert a negative feedback effect on the hypothalamus and anterior pituitary, effectively starving out follicles which did not acquire LHR in the GC layer. Estradiol is known to have a biphasic effect, meaning at low concentrations, its effects are different than at high concentrations [37]. As concentrations increase, finally a threshold is reached which causes the LH surge and ultimately ovulation.

In sheep, true dominance of one follicle over another probably does not occur, as often times more than one follicle will ovulate. However, there are differences between follicles that ovulate (dominant) and those that do not (subordinate), in steroidogenic capacity, diameter, and ability to express *LHR* in the granulosa cell layer [38]. Evans et al. (2002), showed that in monovulatory sheep, when the largest follicle is ablated, the next largest follicle will continue to grow, rather than succumb to atresia [35]. Thus, in monovulatory sheep breeds follicular dominance does occur.

Gonadotropins

Gonadotroph cells are located in the anterior pituitary, and are responsible for the synthesis and release of the pituitary gonadotropins, LH and FSH. Gonadotropins are large

glycoprotein hormones that share sequence homology among α subunits, but differ in β subunit composition. It is the β subunit that determines the biological activity of the hormone.

The mature α subunit, common among several members of the glycoprotein hormone family, consists of 92 amino acids [39]. The α subunit is encoded by a single gene that has four exons. The α protein has 10 cysteine residues that are involved in intrasubunit disulfide bonds. Two Asparagine residues (located within glycosylation consensus sequences) serve as sites for N-Linked glycosylation, which contribute to hormone half-life [40]. Transcription of the α subunit is controlled by the pulse frequency of GnRH, with faster pulses causing a higher rate of α subunit transcription [41].

Pulse frequency of GnRH also controls the rate of transcription of gonadotropin beta subunits. It is thought that low pulse frequency of GnRH favors transcription of the FSH- β subunit, while increased pulse frequency favors LH- β transcription, as reviewed by [41]. Transcriptional control of *FSH* is also controlled by activin, follistatin, and inhibin. Activin and follistatin act through the type II activin receptor (ActRII); inhibin acts through the transforming growth factor- β (TGF- β) receptor to sequester ActRII and prevent its binding to activin or follistatin. Inhibin is produced by growing follicles on the ovary, and acts in an endocrine manner by exerting negative feedback on gonadotroph cells of the anterior pituitary and decreasing FSH production [35]. Activin increases FSH production by binding to the activin receptor-like kinase 4 (ALK-4; type I receptor) on gonadotroph cells to stimulate the transcription factors Smad3 and 4. Activin is negatively regulated by Smad7, which is upregulated by Smad3 and/or 4; activin is also capable of decreasing its own production (and subsequently that of FSH) by binding to ActRII on folliculostellate cells, which increases production of follistatin. Follistatin decreases FSH production both by binding to activin and the

ActRII, each of which would prevent phosphorylation of ALK-4, and eventual transcription of FSH- β (as reviewed by [42]).

Gonadotropin Receptors

The gonadotropin receptors are glycoprotein hormone receptors that belong to the G protein-coupled receptor (GPCR) superfamily, specifically, the family of rhodopsin-like receptors. The luteinizing hormone receptor (LHR), follicle stimulating hormone receptor (FSHR), thyrotropin stimulating hormone receptor (TSHR) and chorionic gonadotropin receptors are all members of the GPCR superfamily. These receptors all contain seven transmembrane segments, and each is thought to interact with guanine nucleotide binding proteins (G proteins) to transduce signaling.

Follicle Stimulating Hormone Receptor Gene

The *FSHR* is approximately 85,000-100,000 base pairs in length and consists of 9 introns and 10 exons [43]. The promoter region of the *FSHR* has been described; however, the specific elements that regulate gene transcription remain an enigma. The strongest promoter activity is located -200 to +163 relative to the transcription start site; the transcription start site is located -163 base pairs relative to the translation start site. No TATA or CCAAT boxes (which are often absent in genes that are constitutively expressed) are found near the transcription start site; however, many potential regulatory elements have been identified. One putative regulatory sequence of interest was a palindrome sequence <GGGTCAC GTGACCC> that was very similar, but not identical, to an estrogen response element. An E-box element was identified, to which upstream stimulatory factor (USF) 1 and 2 were shown to bind [44]. A GT/CACC box

was also identified; zinc finger proteins could potentially bind to this site. Two possible CRE-like elements were found at -1473 to -1466 and -673 to -666, relative to the translation start site. CRE elements serve as a binding site to the *trans*-acting transcription factor CREB, which is activated by increased intracellular levels of cAMP. An AP-1 binding site was identified -1483 to -1491, and an AP-1 reverse binding site was found at -1807 to -1799 bp. Several testes-specific motifs were found, including a Y box type, PuF, AABS, and C mos like elements. These motifs are thought to be important in maintaining testes-specific expression. No elements were identified that might be ovary-specific. Factors that are known to increase expression of *FSHR* include FSH, cAMP, activin, and transforming growth factor- β (TGF- β), while transforming growth factor- α decreases *FSHR* expression [45].

Follicle Stimulating Hormone Receptor Structure

The *FSHR* was first cloned and sequenced in 1990 [6] by screening a rat Sertoli cell cDNA library. Using the same procedures, Yarney et al. (1993), cloned ovine *FSHR* mRNA from a sheep Sertoli cell library [5]. The ovine FSHR is 2431 nucleotides in length, and codes for a protein consisting of 695 amino acids (the first 18 residues code for the signal peptide; the mature protein is 675 amino acids in length; [6]). The FSHR is composed of three domains: an extracellular ligand binding domain, a domain with seven membrane spanning segments, and an intracellular domain. The extracellular ligand binding domain is large and has 348 amino acid residues with three N-linked glycosylation sites [6]. Glycosylation is thought to convey protection from degradation in the extracellular environment, and may be involved with hormone binding and activation of the receptor. The membrane spanning domain consists of 264 residues, and serves to anchor the receptor into the cell membrane. Amino acids which span the

membrane (about 23 amino acids per membrane spanning segment) are arranged in an alpha helical manner. Amino acids that connect the membrane spanning segments form loops that protrude either intra- or extra-cellularly; intracellular loops are important for interaction with G proteins, while extracellular loops may be involved in hormone binding and/or activation of the receptor [46]. The FSHR is thought to preferentially associate with Gs proteins[46]. The intracellular domain has 63 amino acids, and also aids in interaction with G proteins that transduce receptor signaling to downstream effectors.

G Proteins

G proteins are intracellular proteins, which associate with the intracellular loops and carboxyl tail of some receptors (as reviewed by [47]). Many G proteins may interact with a single receptor. There are both stimulatory (Gs) and inhibitory (Gi) G proteins, and monomeric and heterotrimeric G proteins. Monomeric G proteins have a single, small α unit. Monomeric G proteins usually interact with growth factor-type receptors. The FSHR associates with heterotrimeric G proteins which have α , β , and γ subunits. The β and γ subunits are permanently bound together, however the α subunit can detach from the complex. The α , β , and γ subunits are bound in the G protein complex until activated by receptor/ligand binding. In its inactive form, the α subunit is bound by guanine diphosphate (GDP). Once activated, GDP is replaced with guanine triphosphate (GTP), by guanine nucleotide exchange factor (GEF). The alpha subunit, with bound GTP, then detaches from the β and γ subunits and activates the effector enzyme adenylyl cyclase, which converts adenosine triphosphate (ATP) to cyclic adenosine monophosphate (cAMP). Increased intracellular levels of cAMP act as a second messenger, and cause activation of Protein Kinase A (PKA). PKA is composed of four subunits, two catalytic

and two regulatory. The regulatory units keep the catalytic units inactive in the absence of cAMP. When increased cAMP is present, cAMP binds the regulatory subunits of PKA and they detach from the catalytic subunits. The catalytic subunits are then active and can phosphorylate many intracellular target proteins. One of the main targets of PKA is the cAMP response element binding protein (CREB), a transcription factor. Upon activation by PKA, CREB increases gene transcription [47].

Cessation of signaling

Adenylyl cyclase will continue to convert ATP to cAMP until GTP is hydrolyzed to GDP. Once hydrolyzed, the α subunit will reassociate with the β and γ subunits. Excess cAMP is degraded by phosphodiesterase, and downstream signaling ceases [47].

Gene Splicing

Genes have both exons or coding sequences, and introns, or non-coding sequences. When DNA is transcribed into RNA, both introns and exons are copied, which yields pre-mRNA. Transcription occurs within the nucleus of the cell, and is initiated when appropriate transcription factors interact with the promoter of the gene. RNA polymerase II is responsible for transcribing DNA into pre-mRNA. Pre-mRNA undergoes splicing to remove introns prior to its translation. Splicing occurs within the nucleus in a spliceosome. Spliceosomes consist of five small nuclear ribonucleoproteins (snRNP) [48]. Each snRNP has 1-2 snRNAs and several proteins. Small nuclear ribonucleoproteins recognize *cis*-acting elements, which allow them to pinpoint exon/intron boundaries, and attach to the elements in a step-wise manner [48]. After assembly, the spliceosome removes introns through two trans-esterification reactions. Introns

are looped out and degraded. Alternative splicing of RNA can also occur, which involves removing exons that contain coding sequences. Removal of specific exons can still result in mRNA that is translated into functional proteins. It is estimated that about 50% of human genes undergo alternative splicing [49]. After splicing, the resulting mRNA is then further processed by addition of a poly-A tail. This tail conveys stability to the mRNA, and delays its degradation as it travels from the nucleus to the rough endoplasmic reticulum to be translated.

FSHR Alternative Splice Variants

When the sheep *FSHR* was identified by screening a sheep Sertoli cell cDNA library [5], Northern blot analysis of *FSHR* mRNA revealed transcripts of different sizes, providing the first evidence that sheep *FSHR* mRNA was able to undergo alternative splicing and produce transcript variants. Once it was apparent that alternative splicing occurred, updated nomenclature was necessary to distinguish each variant from another; the G protein-coupled form of the receptor became known as FSHR-1.

The first alternatively spliced transcript to be identified and described was HK201 (later renamed FSHR-2 [5]). The FSHR-2 consists of 652 amino acids [5, 50]. The FSHR-2 has high sequence homology with FSHR-1. The sequence for FSHR-2 is the same as FSHR-1 until it diverges at amino acid residue 625, at which point, the sequence differs for the last 27 residues. Exons 1-9 are the same for FSHR-1 and FSHR-2 however, FSHR-2 has a truncated exon 10 spliced to a putative exon 11 [50]. The truncation in exon 10 is thought to affect receptor signaling. Although FSHR-2 has been shown to bind FSH with high affinity, downstream signaling did not occur [8]. In fact, when FSHR-2 and FSHR-1 were cotransfected into HEK 293 cells and treated with FSH, only a small increase in intracellular cAMP was detectable, in

contrast to the large increase normally caused by FSHR-1. These researchers speculated that FSHR-2 attenuated the actions of FSHR-1, leading the authors to conclude that FSHR-2 acts as a dominant negative form of the FSHR [8].

Another alternatively spliced transcript called HK18 (later renamed FSHR-3) was described around the same time [7]. FSHR-3 is composed 259 amino acid residues. The first 223 amino acid residues are identical to the G protein-coupled form of the receptor, with the final 36 residues differing from FSHR-1 [7]. It is of note that these 36 residues do correspond to the carboxy terminus of FSHR-2 [50]. The FSHR-3 shares exons 1-8 in common with FSHR-1, and is spliced at nucleotide 392; exons 9 and 10 are removed and a putative exon 11 is added. Because the extracellular domain of the well-characterized G protein-coupled form is encoded by exons 1-9, and the majority of the domain is present in exons 1-8, FSHR-3 has many of the leucine rich repeats that are needed for hormone binding; thus, FSHR-3 is capable of binding FSH with high affinity [9].

Although FSHR-3 is lacking exon 10, which codes for the seven transmembrane domains that are the hallmark of G protein-coupled receptors, in several different transfection studies FSHR-3 was shown to be expressed at the cell surface [9, 51, 52]. Apparently, the single transmembrane domain encoded by exon 11 is sufficient for insertion into the plasma membrane. It was because of the single transmembrane domain, and the signal transduction pathways activated by FSHR-3, that it was placed into the growth factor type 1 receptor class.

In contrast to FSHR-1, FSHR-3 is thought to act in a cAMP-independent fashion. When stimulated by FSH, it has been shown to activate a mitogen-activated protein kinase (MAPK) pathway, specifically the extracellular-regulated kinase (ERK) signaling cascade [52]. The ERK cascade is involved in cell proliferation and is regulated by Ras. The ERK cascade consists of

three kinase modules: a mitogen-activated protein kinase (MAPK), which is activated by a MAPK/ERK kinase (MEK), which is subsequently activated by another MEK kinase (MEKK). The ERK cascade consists of Raf isoforms ERK1/ERK2 and MEK1/2. Experiments done by Babu et al. (2000), illustrated the activation of the ERK cascade by FSHR-3 is Ca^{2+} dependent [52]. Touyz et al. (2000), showed that activation of FSHR-3 cause a dramatic increase in Ca^{2+} in transfected HEK 293 cells [51]. This calcium increase was thought to be mediated by L-type voltage dependent calcium channels. The significance of these findings relates to the increases in cell proliferation that were observed shortly after calcium influx and activation of the ERK signaling cascade. These studies illustrate that FSH is likely to stimulate cell proliferation directly through FSHR-3.

Seasonality

Sheep are short-day breeders, and have a breeding season which extends from September through February. Ambient day length is important to maintain the circannual rhythm of the breeding season. Maintaining a specific seasonal breeding period from year to year ensures that offspring will be born during a time in which conditions are optimal for survival.

Day length has a direct impact on the secretion of the hormone melatonin [53]. Melatonin is produced by the pinealocytes of the pineal gland, and is only synthesized and secreted during periods of darkness. Melatonin actively determines the reproductive response to photoperiod by stimulating the hypothalamus to increase secretion of GnRH [54, 55]. During the summer months when day length is long, melatonin secretion is negatively inhibited [54]. This inhibition is enacted primarily by non-visual light-sensitive ganglia within the retina.

Darkness and light are perceived by the retina. The retina receives more excitatory stimulation when periods of light are long; this stimulation is transmitted to the suprachiasmatic nucleus region (SCN) of the hypothalamus via the retinohypothalamic tract, (as reviewed by [56]). The SCN transmits the stimulus to the preganglionic neurons of the superior cervical ganglion. This causes postganglionic neurons to fire and excite inhibitory neurons in the pineal gland which inhibit pinealocytes from secreting melatonin. Decreased melatonin secretion causes the hypothalamus to be more sensitive to the negative feedback of estradiol; the hypothalamus responds by secreting less GnRH, and the pituitary by secreting less LH [53]. Circulating progesterone concentrations decrease after the last luteal phase of the breeding season. Remarkably, secretion of FSH remains robust during the transition to anestrus; however, it appears that the ovary becomes less sensitive to gonadotropin stimulation [57]. Ewes still develop follicles on the ovary during the anestrous period, however, emergence of follicular waves does not result in higher levels of circulating estrogen [57].

As the hours of light begin to shorten during the months of autumn, the retina receives fewer excitatory stimuli. Negative inhibition of pinealocytes diminishes, and allows increased secretion of melatonin. In addition, the hypothalamus becomes less sensitive to the negative feedback of estradiol, and cyclicity resumes.

When transitioning into the breeding season, the first ovulation is not accompanied by estrous behavior. Progesterone priming of the hypothalamus is necessary before estrous behavior will be displayed. The CL that results from the first ovulation of the breeding season is often sub-normal, but is sufficient to prime the hypothalamus, and estrous behavior is displayed before the second ovulation.

Various protocols have been established to stimulate fertile ovulations during the transition to anestrous or anestrous periods of sheep. One of the most widely used protocols in Australia and New Zealand uses a controlled internal drug releasing (CIDR; EAZI-BREED CIDR protocol) progesterone insert followed by injection with PMSG (400-500 IU). The CIDR is inserted for 14 days to simulate a luteal phase, prime the hypothalamus, and increase GnRH pulse frequency. The PMSG is given on day 14 at CIDR removal; PMSG functions as surrogate gonadotropin support for growing follicles, similar to that of FSH, but with longer half-life in circulation. This protocol induces estrus and fertile ovulations about 54 hours after CIDR removal/PMSG injection.

CHAPTER 2 - EXPRESSION OF FOLLICLE STIMULATING HORMONE RECEPTOR VARIANTS DURING THE ESTROUS CYCLE OF SHEEP

Introduction

For successful reproduction to occur, follicles must develop and grow within the ovary. Antral follicle growth is regulated largely by the pituitary gonadotropins follicle stimulating hormone (FSH) and luteinizing hormone (LH). In order for gonadotropins to exert their effects, the appropriate receptors must be present at the correct time. Follicle stimulating hormone receptor (FSHR) is detectable soon after follicle formation in sheep [13]. Several alternatively spliced *FSHR* mRNA variants have been identified in sheep [5, 7, 13, 50]. Each splice variant has a unique exon structure which may dictate receptor coupling to signaling molecules. Messenger RNA for the G protein-coupled form of the *FSHR* (hereafter referred to as FSHR-1) was first described in the rat in 1990 [6] and in the sheep in 1993 [5]. Sheep FSHR-1 mRNA is 2431 base pairs (bp) in length, and consists of 10 exons. Once translated, FSHR-1 is capable of activating several intracellular signaling pathways, but cAMP/PKA is the most commonly described pathway (as reviewed by [58]). The FSHR-1 is important for granulosa cell (GC) differentiation and hormone production, as well as GC proliferation (as reviewed by [59]). Other identified splice variants include FSHR-2 (dominant negative receptor) and FSHR-3 (growth factor type-1 receptor).

The exon structure of FSHR-2 is similar to that of FSHR-1, except that FSHR-2 has a truncated exon 10 spliced to exon 11 [50]. The truncation in exon 10 is thought to affect

receptor signaling. Although FSHR-2 has been shown to bind FSH with high affinity, downstream signaling did not occur [8]. In fact, when FSHR-2 and FSHR-1 were cotransfected into HEK 293 cells and treated with FSH, only a small increase in intracellular cAMP was detectable, in contrast to the large increase normally caused by FSHR-1. Thus, FSHR-2 appeared to attenuate the actions of FSHR-1, leading the authors to conclude that FSHR-2 acts as a dominant negative form of the FSHR [8].

Exons 1-8 of FSHR-3 are identical to that of FSHR-1; however, FSHR-3 lacks exons 9 and 10, and is spliced to exon 11 [7, 9]. In contrast to FSHR-1, FSHR-3 is thought to act in a cAMP-independent fashion. When stimulated by FSH, it has been shown to activate a mitogen-activated protein kinase (MAPK) pathway, specifically the extracellular-regulated kinase (ERK) signaling cascade [52]. The ERK cascade is involved in cell proliferation and is regulated by Ras; activation of the ERK cascade is Ca^{2+} dependent. When Touyz et al. (2000) transfected HEK 293 cells with FSHR-3, treatment with FSH resulted in a dramatic increase in Ca^{2+} [51]. The significance of these findings relates to the increases in cell proliferation observed shortly after calcium influx and activation of the ERK signaling cascade. These studies illustrate that FSH can stimulate cell proliferation directly through FSHR-3.

In the cow, *FSHR* transcripts containing exon 11 are more highly expressed in cohort and subordinate follicles compared to dominant follicles. However, *FSHR* transcripts containing exon 10 are more highly expressed in cohort and dominant follicles than in subordinate follicles during the estrous cycle [60, 61]. Based on those findings, we postulated that in sheep, transcripts in addition to FSHR-1 may act in a concerted fashion to cause follicular growth and atresia. The aim of these experiments was to determine the expression patterns of *FSHR* variants

during the estrous cycle under normal physiological conditions, and to determine if treatment with PMSG altered expression patterns.

Materials and Methods

Animals and Sample Collection

All animal procedures were approved by the Kansas State University Animal Care and Use Committee (IACUC #2735). Ewes were group housed outside at the KSU Sheep Unit in a south-facing lean-to barn and were exposed to natural lighting and temperature (39° 12' 22" N, 96° 35' 12" W). Ewes had free access to water and were fed a maintenance diet of grass hay and 2 pounds/head/day of a grain supplement (87% DM; 14% CP; 85% TDN). Ewes were transported from the KSU Sheep Unit to the KSU Diagnostic Lab for euthanasia. When ewes were loaded onto the trailer, blood samples were collected via jugular venipuncture and placed on ice until refrigeration at 4°C for 24 hours. Serum was separated by centrifugation at 1500xg for 20 minutes at 4°C. Serum was decanted into a 5 ml polypropylene tube, capped and stored at -20°C until assay. Time from loading ewes to euthanasia was less than 1 hour. Ewes were euthanized by intravenous overdose (90mg/kg) of sodium pentobarbital.

Experiment 1: Eight mature cycling (2-8 years of age) Suffolk-cross ewes were allowed to come into estrus naturally. Estrous cycle length was monitored through 3 cycles before harvesting ovaries at the end of the breeding season, starting on January 23, 2009, and ending on February 3, 2009. Cyclicity was monitored using a HeatWatch® detection system (Denver, CO) and two vasectomized rams. Onset of estrus was defined as the beginning of the period that a ewe was receptive to mounting by the ram. After a HeatWatch® transmitter was activated by a ram, estrus behavior was visually confirmed. Ewes were euthanized 24 (n=3), 36 (n=3), or 48

(n=2) hours after onset of estrus. Ovaries were harvested and placed on ice before transport to Weber Hall for evaluation. Left and right ovaries of each ewe were kept separate until photographed and all ovarian structures were measured (to the nearest 0.5 mm) and recorded. Ovarian structures were measured with a transparent ruler from the external surface of the ovary. All visible follicles were aspirated using 1cc syringes and 20 gauge needles. Each follicle was aspirated such that the needle was inserted, follicular fluid was pulled into the syringe and then pushed back into the same follicle three times before removing the needle and moving to the next follicle. A new syringe and needle were used for each ewe and each follicle size class. Aspirates were pooled in 1.5 ml microcentrifuge tubes according to follicular diameter: small (≤ 2.0 mm), medium (2.1-4.0 mm) large (4.1-6.0 mm) and preovulatory (≥ 6.1 mm). Follicular fluid and granulosa cells were separated by centrifugation at room temperature for two minutes at 2300xg. Follicular fluid was removed and stored at -20°C for estrogen and progesterone assays.

Granulosa cell pellets were resuspended in 500 μl ice-cold Dulbecco's Phosphate Buffered Saline (PBS; Invitrogen, Carlsbad, CA), then centrifuged at room temperature for one minute at 2300xg. The PBS was aspirated and discarded and the granulosa cell pellets were resuspended in 1 ml TRIzol[®] reagent (Invitrogen) and frozen at -20°C until all samples were collected. Time between ovary harvest and placing granulosa cells in TRIzol[®] reagent did not exceed 2 hours.

Experiment 2: Seven mature (ages 1-8) Suffolk-cross ewes received controlled internal drug-releasing (CIDR; EAZI-BREED[™] CIDR[®], Pfizer New Zealand, Mt. Eden, Auckland) progesterone inserts for 14 days (beginning on February 9, 2009), followed by treatment (n=3) with pregnant mare serum gonadotropin (PMSG, 500IU; SIGMA, St. Louis, MO), or no PMSG (n=4; CIDR only). Ewes were euthanized 24 (n=4; 2 CIDR-only, 2 PMSG-treated), or 36 (n=3;

2 CIDR-only, 1PMSG treated) hours after CIDR removal. All other procedures are the same as for Experiment 1.

RNA Isolation and DNase Treatment

RNA was isolated from samples using TRIzol® reagent according to the manufacturer's instructions (protocol in Appendix A). The RNA pellet was washed with 75% EtOH and resuspended in 15 µl preheated (65°C) nuclease-free water (Ambion®, Austin, TX). All RNA extracts were treated with TURBO DNA-free™ (DNase; Ambion®) according to the manufacturer's instructions (protocol in Appendix A) to remove any genomic or other cellular DNA and stored at -20°C.

Reverse Transcription – Polymerase Chain Reaction

Total RNA (100 ng) was used as starting template for RT-PCR. Some samples with low ($\leq 50\text{ng}/\mu\text{l}$) concentrations of total RNA initially failed to produce consistent real-time PCR products. Total RNA from those samples was then reverse-transcribed using 200 or 300 ng RNA. Samples that required $\leq 0.4 \mu\text{l}$ total RNA to be pipetted were diluted 1:10, and 10 times the diluted amount was used, contributing 8 µl of a 20 µl total reaction volume. Total RNA was reverse-transcribed using SuperScript™ III First-Strand Synthesis SuperMix (Invitrogen), according to the manufacturer's instructions (protocol in Appendix A). Conditions were as follows for reverse transcription: 25°C hold for 25 minutes, 42°C for 50 minutes, 85°C for 5 minutes. At the end of the reverse-transcription reaction, samples were placed on ice for at least 1 minute. To remove template RNA, 1 µl RNase H was added to each sample and samples were incubated at 37°C for 20 minutes. Reactions were stored at -20°C until used for qPCR.

Real-Time Polymerase Chain Reaction

Real-time PCR was performed using an ABI 7500 Fast machine (Applied Biosystems, Foster City, CA) with the following parameters: 50°C for 2 min hold, 95° for 2 min hold, 40 cycles of: 95°C for 15 sec, 60°C for 30 sec. Platinum® SYBR® Green qPCR SuperMix-UDG (Invitrogen™, Carlsbad, CA) was used at 10 µl per well; forward and reverse primers were used at 250 nM concentrations, cDNA template was diluted in 5 µl total volume using nuclease-free water, and nuclease-free water was used to bring the final reaction volume to 20 µl. Melt-curve analysis was performed on all samples after amplification, by heating products to 95°C and plotting the derivative of the reporter (fluorescence) and temperature at which products denature (separation of products prevents fluorescence). All primers were designed using Primer Express® 3.0 software (Applied Biosystems) and synthesized by Applied Biosystems. Beta-Actin was used as an internal standard. Primers used to detect (Table 2.1) FSHR-1, FSHR-2, and FSHR-3 were designed to amplify each variant specifically, based on submitted nucleotide sequences of each variant (Figures 2.1-2.3).

Target	Accession No.	Primer Name	Sequences 5' to 3'	Primer (bp)	Amplicon (bp)
Beta-Actin	NM_001009784	oBeta-Actin Forward	GTCATCACCATCGGCAATGA	20	88
		oBeta-Actin Reverse	CGTGAATGCCGCAGGATT	18	
FSHR-1	L07302	oExon 10-1 Forward	CATTCACTGCCCACTTTTCATC	24	84
		oExon 10-1 Reverse	TGAGTGTGTAATTGGAACCATTGGT	25	
FSHR-2	NM_001009289	oExon 10/11-1 Forward	CAGGAACTTCCGCAGGGATT	20	72
		oExon 10/11-1 Reverse	TGATTGCAGATGAGCCCAACA	21	
FSHR-3	L12767	oExon 8/11-0 Forward	CAGTAATTTGGAAGAAGTGCCTAATG	26	80
		oExon 8/11-0 Reverse	AACAGTGCAGCAGTGGAGACA	21	
LHR	L36329	oLHR Forward	AGATTGCTAAGAAAATGGCAGTCCTCT	28	82
		oLHR Reverse	GCAGCTGAGATGGCAAAGAAAGAGA	25	

Table 2.1. Description of primers used for quantitative real-time PCR.

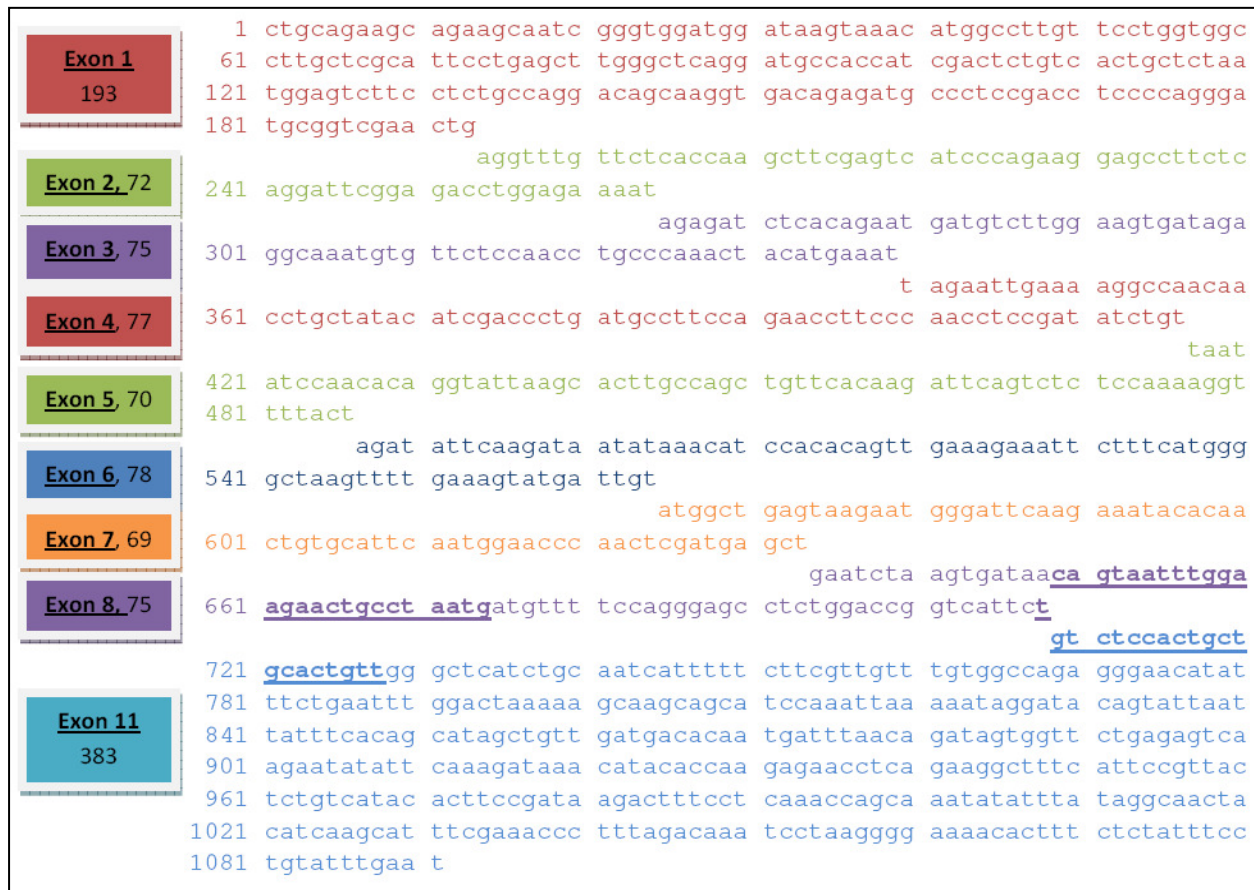


Figure 2.1. Nucleotide sequence and exon structure for FSHR-3.

The FSHR-3 mRNA (accession No. L12767) consists of exons 1-8 spliced to exon 11, and is 1091 nucleotides (nt) in length. Exon numbers and nt per exon are denoted in the colored boxes along the left side of the figure. Primers for real-time PCR, designed with Primer Express[®] 3.0 software, were constructed to span exons 8 and 11 so that only FSHR-3 and neither FSHR-2 (which contains exons 9 and 10) nor FSHR-1 (which lacks exon 11) would be amplified. Annealing sites for the exon 8/11 primer pair are bold and underlined. The expected amplicon would start at nt-658 and extend through nt-728 (80 nt in length).



Figure 2.2. Nucleotide sequence and exon structure for FSHR-2.

The FSHR-2 mRNA (accession No. NM_001009289) consists of exons 1-9 and a truncated exon 10 spliced to exon 11, and is 2428 nucleotides (nt) in length. Exon numbers and nt per exon are denoted in the colored boxes along the left side of the figure. Primers for real-time PCR, designed with Primer Express[®] 3.0 software, were constructed to span exons 10 and 11 so that only FSHR-2 and neither FSHR-3 (which lacks exons 9 and 10) nor FSHR-1 (which lacks exon 11) would be amplified. Annealing sites for the exon 10/11 primer pair are bold and underlined. The expected amplicon would start at nt-2011 and extend through nt-2082 (72 nt in length).



Figure 2.3. Nucleotide sequence and exon structure for FSHR-1.

The FSHR-1 mRNA (accession No. L07302) consists of exons 1-10, and is 2431 nucleotides (nt) in length. Exon numbers and nt per exon are denoted in the colored boxes along the left side of the figure. Primers for real-time PCR, designed with Primer Express® 3.0 software, were constructed to reside within the latter part of exon 10 so that only FSHR-1 and neither FSHR-2 (which is truncated at nt 2045 of exon 10) nor FSHR-3 (which lacks exons 9 and 10) would be amplified. Annealing sites for the exon 10 primer pair are bold and underlined. The expected amplicon would start at nt-2097 and extend through nt-2180 (84 nt in length).

RIA

Duplicate aliquots (50 µl) of serum were assayed for progesterone concentration, as described and validated previously [62]. Sensitivity of the assay was 3.5 pg/tube and the mean intra- and inter-assay coefficients of variation (CV) were 4.75% and 4.55%, respectively.

Duplicate aliquots (200 µl total volume) of follicular fluid were assayed without extraction for estradiol and progesterone, using previously described and validated assays [63, 64] (protocols in Appendix A). Briefly, for estradiol evaluation, follicular fluid from small and medium-sized follicles was diluted 1:100 and follicular fluid from large and preovulatory follicles was diluted 1:500 prior to assay. Estradiol concentration was determined using a double antibody kit from Siemens Medical Solutions Diagnostics (Deerfield, IL). Sensitivity of the assay was 0.02 pg/tube and the mean intra-assay CV was 1.6%. Progesterone concentrations were determined using Coat-A-Count antibody coated tubes from Siemens Medical Solutions Diagnostics. For progesterone evaluation, follicular fluid from all follicle sizes was diluted 1:50. Sensitivity of the assay was 0.012 ng/tube and the mean intra-assay CV was 9.35%.

Statistical Analysis

Relative Expression ($2.0^{-\Delta C_t} \times 1000$) values were used for statistical analysis of real-time PCR data. Data were analyzed with SAS 9.1 software (SAS Institute, Cary, NC) using Proc Mixed and least squared means. Both experiments had a completely randomized design with a split-plot; for both experiments, the split-plot has treatments in a 2 (follicle size) x 4 (gene) factorial. The ANOVA models included all treatment factor main effects and interactions; ewe was included as a random effect. Normality of residuals was tested and data transformed if necessary. For Experiment 1, the whole-plot treatment factor is hour and experimental unit is ewe. Gene expression in preovulatory follicles was analyzed separately because this size was

only present in the 24 hour group. Untransformed data are presented as least squared means of relative expression, \pm SEM. For Experiment 2, the whole-plot treatments are in 2 (hour) x 2 (treatment) factorial and the whole-plot experimental unit is ewe. Data were (natural) log transformed to achieve normality. After least squared means were calculated, they were back-transformed (by exponentially raising the transformed mean values). Confidence intervals for the transformed means were calculated so new standard errors could be assigned. Back-transformed data are presented as least squared means of relative expression, \pm SEM. Data for the large follicle size class could not be statistically analyzed, as this size was only found in one ewe from the 24 hour PMSG group and one ewe from the 36 hour control group. Therefore, relative expression from the large follicle group are presented as raw data.

Analysis of Techniques

RNA Quantitation

After DNase treatment, RNA was quantified with a Nanodrop 1000 Spectrophotometer (protocol in Appendix A) to determine RNA quantity at 260 nm. All RNA was diluted 1:3 before quantitation (2 μ l RNA was diluted in 4 μ l nuclease-free water) and analyzed in duplicate with the Nanodrop; DNase buffer was used as the blank calibrator. The quantity of RNA in each sample was confirmed at the same time that quality of the RNA was examined using an Agilent 2100 Bioanalyzer with an Agilent 6000 Nano Kit (Agilent Technologies, Waldbronn, Germany). The Nano chip was prepared according to the manufacturers instructions (protocol in Appendix A). Briefly, 1 μ l total RNA (undiluted) and marker (5 μ l; marker is used to equalize loading; 6 μ L total reaction volume) was loaded into a gel-dye matrix in an Agilent 6000 Nano chip (Agilent Technologies). A 6000 nucleotide (nt) RNA ladder (6 μ l) was used for size

comparison; each chip (12 samples) was electrophoresed using the Agilent 2100 Bioanalyzer and the eukaryotic total RNA program settings.

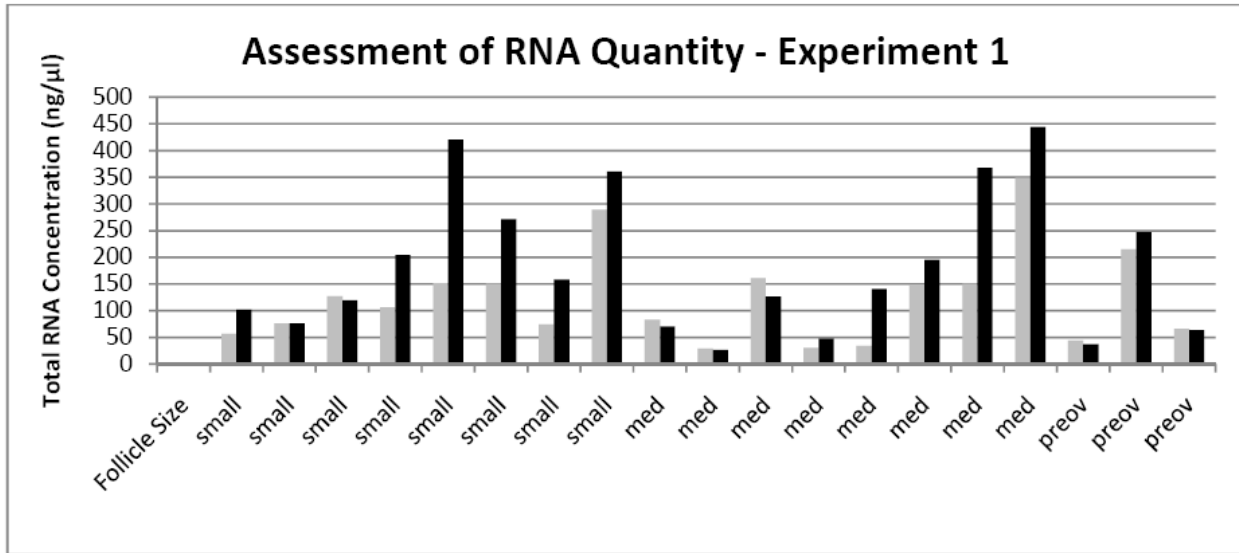


Figure 2.4. Comparison of quantitation methods after extraction of total RNA— Experiment 1.

Granulosa cells were collected from ewes 24, 36 or 48 hours after the onset of estrus and pooled according to follicle diameter: small (≤ 2.0 mm), medium (2.1-4.0 mm) and preovulatory (preov; ≥ 6.1 mm). Total RNA was extracted with TRIZol reagent and then subjected to DNase treatment (Turbo DNA-free; used for blank measurement). Total RNA was quantified by loading 1 μ l total RNA (undiluted) onto an Agilent 6000 Nano chip and reading with an Agilent 2100 Bioanalyzer (gray bars), which uses fluorescence to quantify RNA. Total RNA was also quantified by loading duplicate aliquots (1.3 μ l) of diluted (1:3) onto the Nanodrop 1000 Spectrophotometer (black bars), which uses absorbance at 260 nm to quantify RNA. Overall, Nanodrop concentrations were higher than Bioanalyzer concentrations, but the two methods were correlated ($R=.83$).

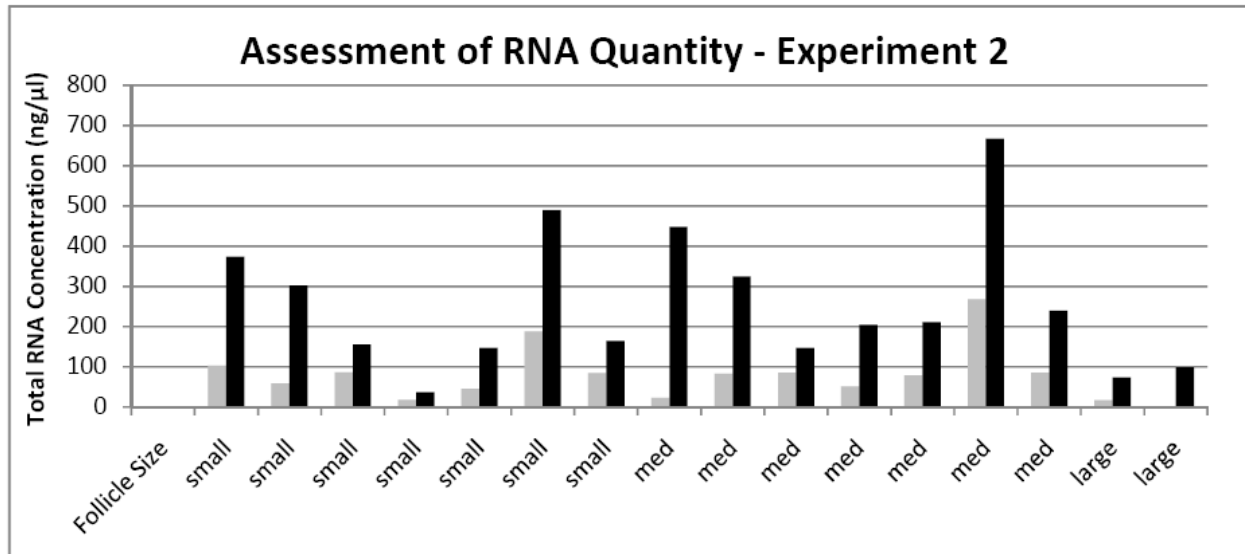


Figure 2.5. Comparison of quantitation methods after extraction of total RNA— Experiment 2.

Granulosa cells were collected from ewes 24 or 36 hours after CIDR removal and pooled according to follicle diameter: small (≤ 2.0 mm), medium (2.1-4.0 mm) and large (4.1-6.0 mm). Total RNA was extracted with TRIzol reagent and then subjected to DNase treatment (Turbo DNA-free; used for blank measurement). Total RNA was quantified by loading 1 μ l total RNA (undiluted) onto an Agilent 6000 Nano chip and reading with an Agilent 2100 Bioanalyzer (gray bars), which uses fluorescence to quantify RNA. Total RNA was also quantified by loading duplicate aliquots (1.3 μ l) of diluted (1:3) onto the Nanodrop 1000 Spectrophotometer (black bars), which uses absorbance at 260 nm to quantify RNA. Overall, Nanodrop concentrations were higher than Bioanalyzer concentrations, but the two methods were correlated ($R=0.79$).

RNA Quality

The RNA quality was assessed on 3-23-09 and 3-24-09 (in the same assay that measured quantity) with the Agilent 2100 Bioanalyzer (Figure 2.6). One sample, (from Ewe 11; 36 hour) containing total RNA from one preovulatory-sized follicle was thrown out after failing to amplify any gene (other than β -actin), in 10 duplicate real-time PCR reactions. The RNA quality of this sample was later shown to be poor (Figure 2.6 C, lane 6). One sample containing medium follicles from Ewe 4 (48 hour; $n=3$ follicles) had an estrogen to progesterone ratio of 2.0, and could therefore be considered a pool of healthy follicles. Interestingly, both FSHR-2 and LHR were not amplified in that sample (even after 4 attempts). RNA quality for that sample was

shown to be poor (Figure 2.6, B, lane 11), but two variants, FSHR-1 and FSHR-3, were still amplified.

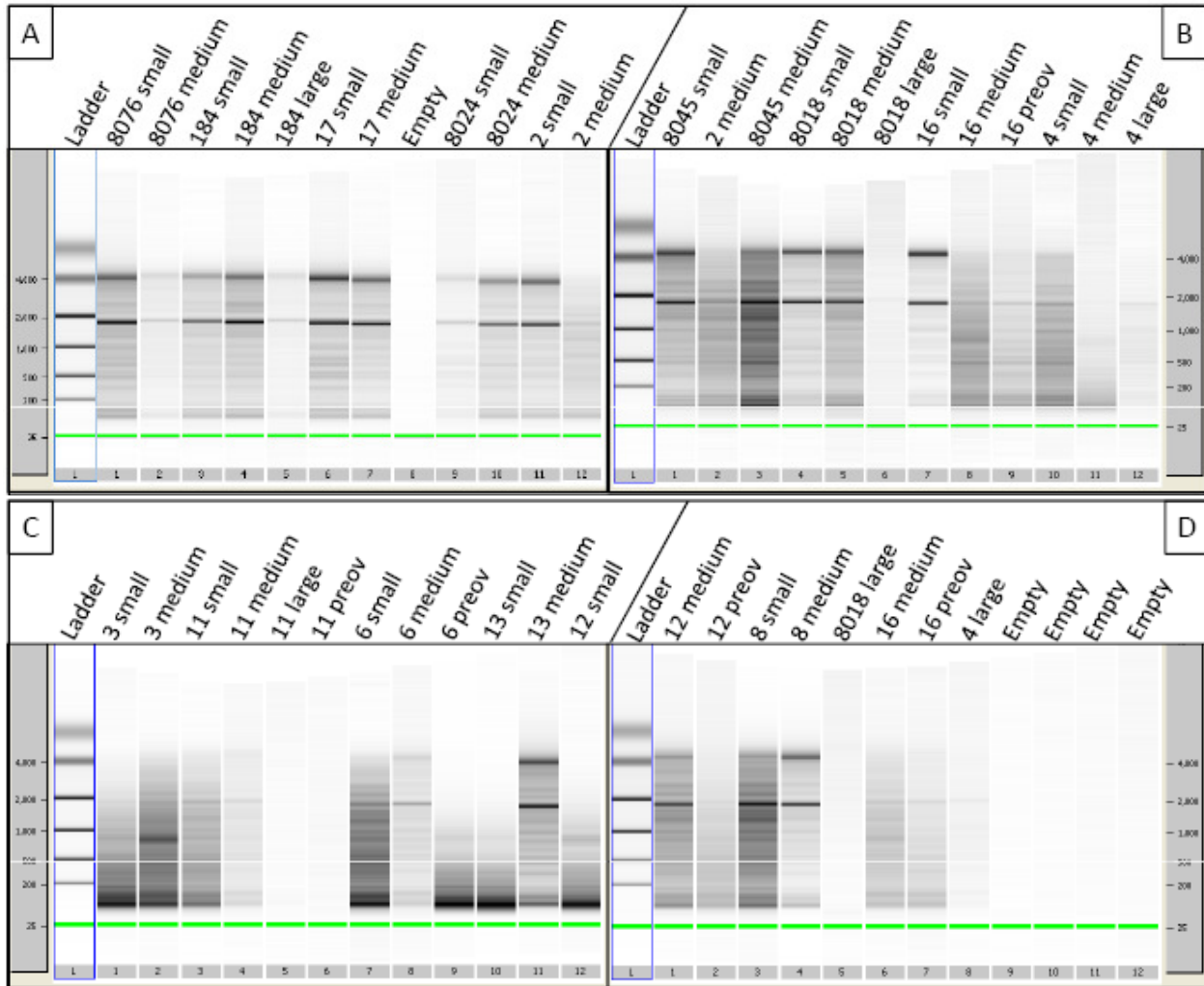


Figure 2.6. Quality assessment of total RNA from sheep granulosa cells.

Total RNA (1 μ l) and marker (5 μ l; marker is used to equalize loading and is seen as the bright green band in each lane; 6 μ L total reaction volume) was loaded into a gel-dye matrix in an Agilent 6000 Nano chip and electrophoresed using the Agilent 2100 Bioanalyzer with the eukaryotic total RNA program settings. A 6000 nucleotide (nt) RNA ladder (6 μ l) was used for size comparison (Lane L, each panel) Ribosomal RNA 18S and 28S bands appear at 1800 and 4000 nts, respectively. Panel A) Samples from Experiment 2: all samples have 18- and 28S bands with the exception of Lane 12. Panel B) Samples from Experiment 2, lanes 1-6; samples from Experiment 1, lanes 7-12; samples in lanes 1, 4, 5 and 7 are of good quality; samples in lane, 9, 10, and 12 have faint 18S bands; samples in lanes 2, 3, 6, 8 and 11 have degraded. Panel C) Samples from Experiment 1: Sample in lane 11 is of good quality; samples in lanes 2, 3, 4, 7 and 8, have 18S bands and some faint 28S bands; samples in lane 5 and 6 have low RNA quantity and thus, quality is difficult to assess; samples in lanes 1, 9, 10, and 12 have degraded. Panel D) Samples from Experiment 1, lanes 1-4; lanes 6-8, reruns; samples in lanes 1, 3, 4, 6, 7

and 8 are good quality; samples in lanes 2 and 5 are degraded. Quality was assessed more than one month after quantitative PCR (qPCR) was completed; samples appeared to degrade over time, as Panel A samples were collected more recently than panel C samples. Quality of RNA was assumed to be similar to that of panel A, lane 11 at the time of qPCR.

Agarose Gel Electrophoresis

Each *FSHR* variant template amplified by real-time PCR was examined by agarose gel electrophoresis (protocol in Appendix A) to examine amplicon size (Figure 2.7, F). Real-time PCR products (30 μ l) and 4 μ l sample buffer were loaded into a 1.5% agarose gel. A 100 bp DNA ladder standard (6 μ l; New England Biolabs, Beverly, MA) and 4 μ l sample buffer was used for size reference. Samples were electrophoresed for 105 volt hours (1.5 hours x 70 volts) then visualized with UV light. Bands were visible for each primer set at the anticipated size.

Melting Curve Analysis

Melting curves were generated for each real-time PCR reaction; examples of melting curves for each primer set are shown in Figure 2.7, A-E, and each appears to show amplification of only one product per primer set.

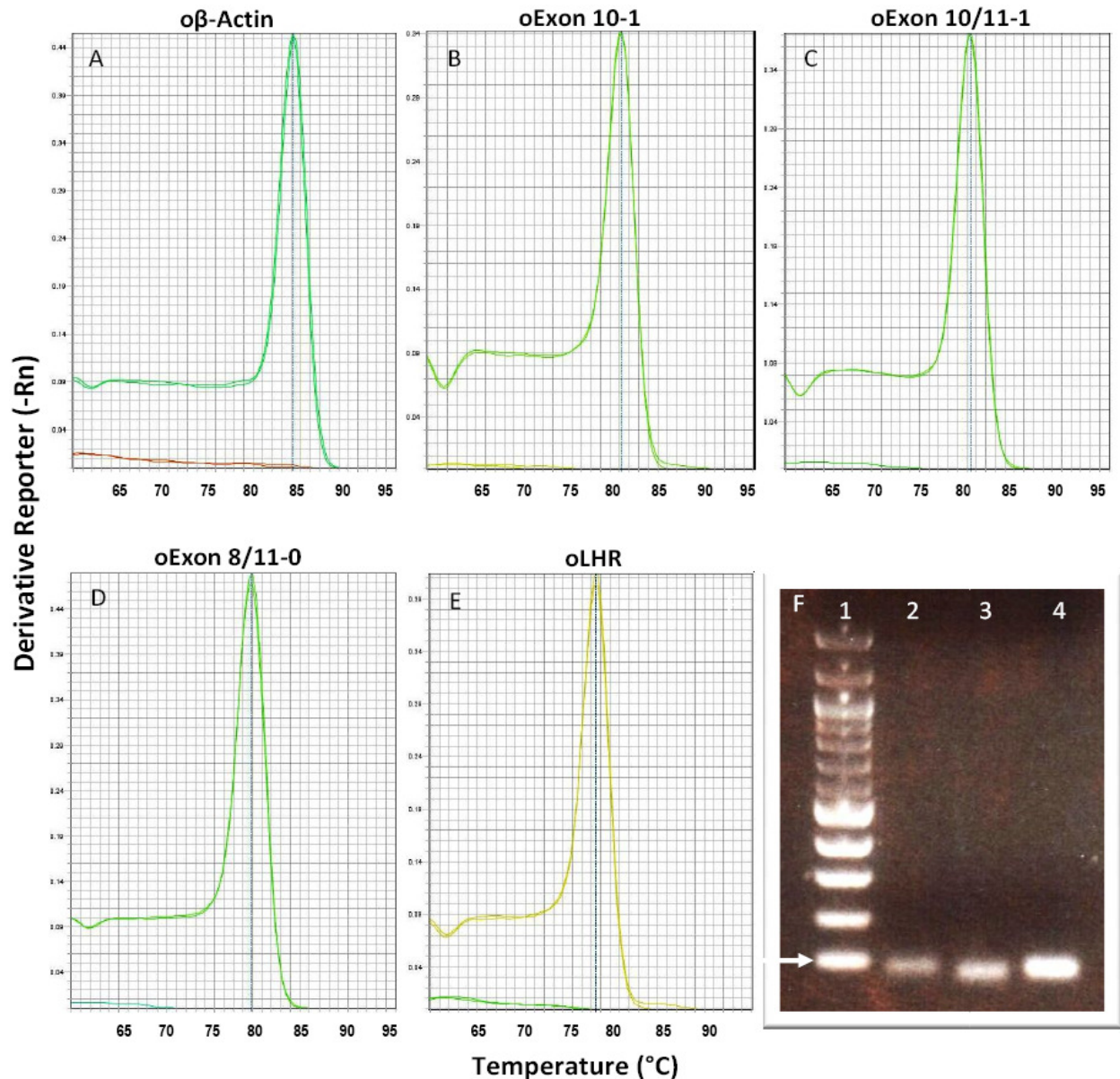


Figure 2.7. Representative melt-curve analysis of primer sets and amplicon size.

Total RNA from sheep granulosa cells was DNase treated and reverse-transcribed, then subjected to quantitative PCR with SYBR Green dye. A-E) Representative melting curves for each primer set (non-template controls for each set appear at bottom left corner of each graph) show only one peak and thus amplification of only one product. Melting temperature of target amplicons ranged from 78.51-84.22°C, and from 62.06-63.83°C for non-template controls. F) Real-time PCR products for *FSHR* variants were electrophoresed in a 1.5% agarose gel with 0.6 μ l ethidium bromide. Lane 1, 100 base pair (bp) DNA ladder standard, white arrow indicates the 100 bp marker; lane 2, *FSHR*-1; lane 3, *FSHR*-2; lane 4 *FSHR*-3. Each reaction produced only one band at the expected size of approximately 84, 72, and 80 bp, respectively. Collectively, evidence provided in panels A-F illustrates that real-time PCR primers were amplifying only the correct targets.

Results

Relative gene expression was determined for both experiments. Primer efficiencies ranged from 85 to 100%. Primer efficiencies under 95% were corrected to 100% so that comparisons between genes could be made. For Experiment 1, when comparing all *FSHR* variants and *LHR* within a follicle class size, *FSHR*-3 was more highly expressed than *FSHR*-1 in medium follicles ($p < 0.01$; Figure 2.8, B), and tended to be higher in small follicles ($p=0.09$). Relative expression of *FSHR*-3 was higher than *FSHR*-2 in small and medium follicles ($p < 0.01$; Figure 2.8, A). In preovulatory follicles, *LHR* expression increased dramatically and was higher than all *FSHR* variants ($p < 0.05$); expression of *FSHR* variants was numerically lower than in small and medium follicles (Figure 2.8 C).

When comparing expression of each variant between small and medium follicles, neither *FSHR*-1 nor *FSHR*-2 was differentially expressed ($p=0.34$ and 0.42 , respectively; Figure 2.9, A, B); however, *FSHR*-3 expression was higher in medium than in small follicles ($p < 0.01$; Figure 2.9, C). Relative expression of *LHR* was essentially undetectable in small follicles and very low, on average, in medium follicles ($p=0.85$; Figure 2.9, D).

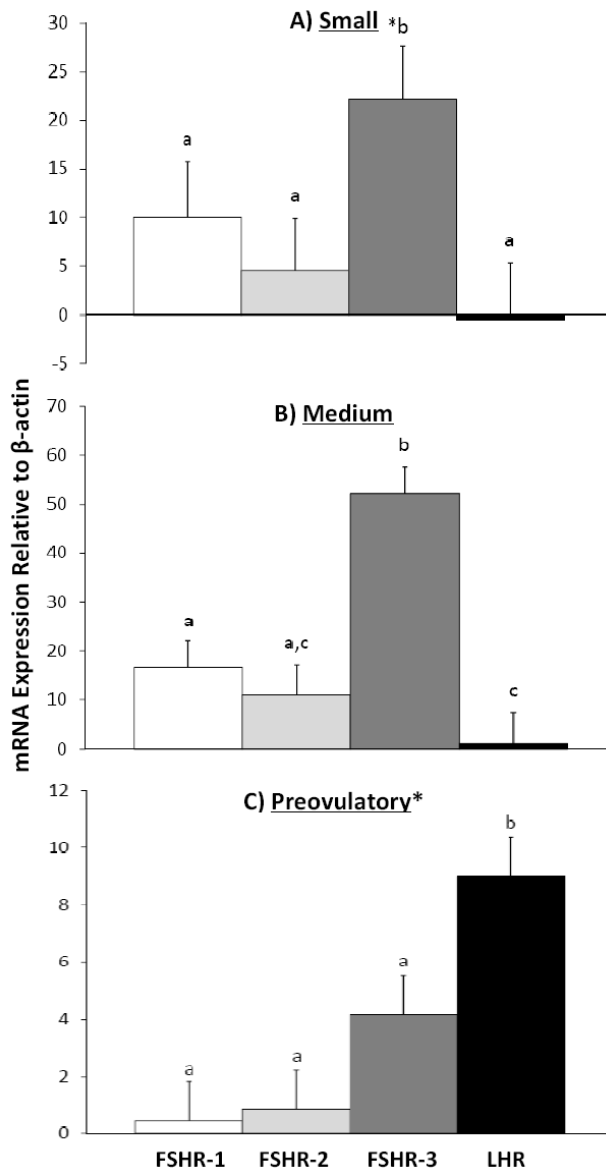


Figure 2.8. Expression of gonadotropin receptors within different sized sheep follicles— Experiment 1.

Granulosa cells were collected from small (≤ 2.0 mm), medium (2.1-4.0 mm) and preovulatory (≥ 6.1 mm;*only found in the 24 hour group) follicles. After total RNA was extracted, it was subjected to reverse transcription and quantitative PCR. Data are expressed as least squared means of relative expression ($2^{-\Delta Ct} \times 1000$; arbitrary units) \pm SEM. Bars within graphs with differing superscripts are different (p \leq 0.05). Expression of FSHR-1 (white bars), FSHR-2 (light gray bars), FSHR-3 (dark gray bars), and LHR (black bars) are compared within a follicle size class. Panel A) Relative expression of FSHR-3 was higher than FSHR-2 and LHR, and tended to be higher than FSHR-1 (*p=0.09) in small follicles. Panel B) Relative expression of FSHR-3 was higher than other variants and LHR in medium follicles. Relative abundance of mRNA for FSHR-1 and FSHR-2 did not differ, but both were more highly expressed than LHR. Panel C) Relative expression of LHR was the highest in preovulatory follicles, while FSHR-1, FSHR-2, and FSHR-3 did not differ.

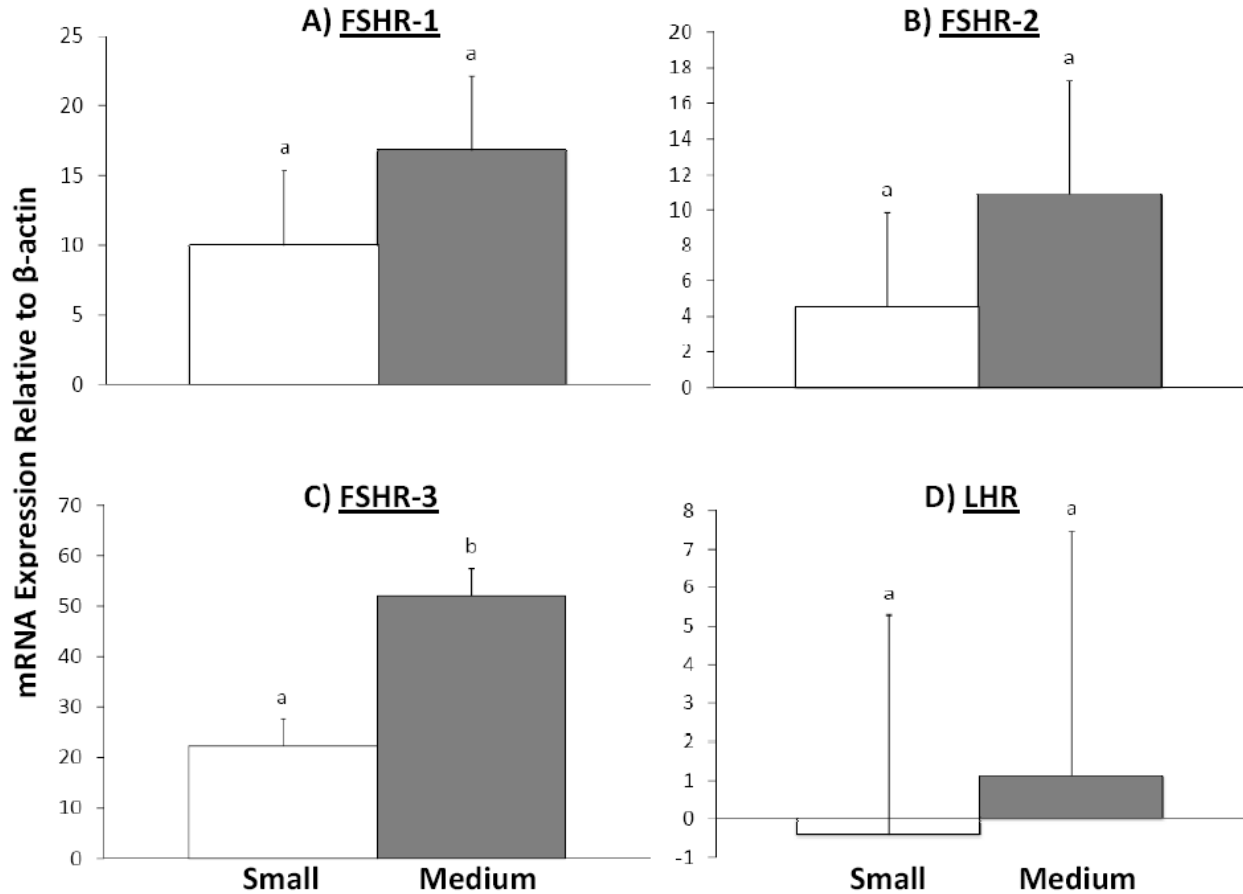


Figure 2.9. Expression of gonadotropin receptors across different sized sheep follicles— Experiment 1.

Granulosa cells were collected from small (≤ 2.0 mm; white bars) and medium (2.1-4.0 mm; gray bars) follicles. After total RNA was extracted, it was subjected to reverse transcription and quantitative PCR. Data are expressed as least squared means of relative expression ($2^{-\Delta Ct} \times 1000$; arbitrary units) \pm SEM. Bars within graphs with differing superscripts are different ($p < 0.01$). Panels A, B, and D) Relative expression of FSHR-1, FSHR-2, and LHR did not significantly differ in small versus medium follicles. Panel C) Relative expression of FSHR-3 was higher in medium than small follicles. Overall, FSHR-3 expression was the only transcript that differed between small and medium follicles.

Experiment 2 real-time PCR results were somewhat different from those in Experiment 1.

When comparing all transcripts within a follicle size, FSHR-1 and FSHR-3 were more highly expressed than FSHR-2 and LHR in small and medium follicles ($p < 0.01$; Figure 2.10 A,B).

When comparing relative expression of each transcript in small or medium follicles, expression of FSHR variants was numerically higher in small than medium follicles ($p > 0.2$); expression of

LHR was higher in small than medium follicles ($p < 0.05$; Figure 2.11, A-D). Relative expression of LHR was higher ($p < 0.05$) in medium than in small follicles (Figure 2.11, D).

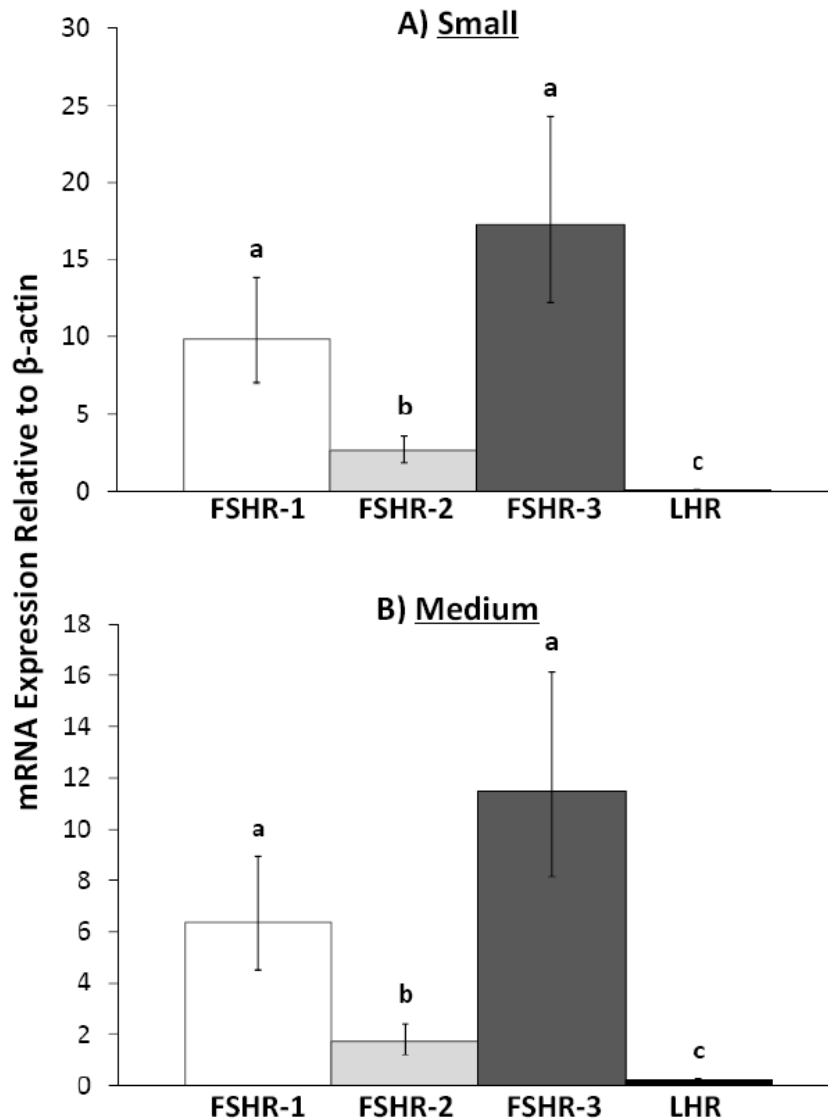


Figure 2.10. Expression of gonadotropin receptors within different sized sheep follicles— Experiment 2.

Granulosa cells were collected from small (≤ 2.0 mm) and medium (2.1-4.0 mm) follicles. After total RNA was extracted, it was subjected to reverse transcription and quantitative PCR. Data are expressed as least squared means of relative expression ($2^{-\Delta Ct} \times 1000$; arbitrary units) \pm SEM. Bars within graphs with differing superscripts are different ($p < 0.01$). Expression of FSHR-1 (white bars), FSHR-2 (light gray bars), FSHR-3 (dark gray bars), and LHR (black bars) are compared within a follicle size class. Relative expression of FSHR-1 and -3 was higher than FSHR-2 and LHR in small follicles and medium follicles (Panels A and B).

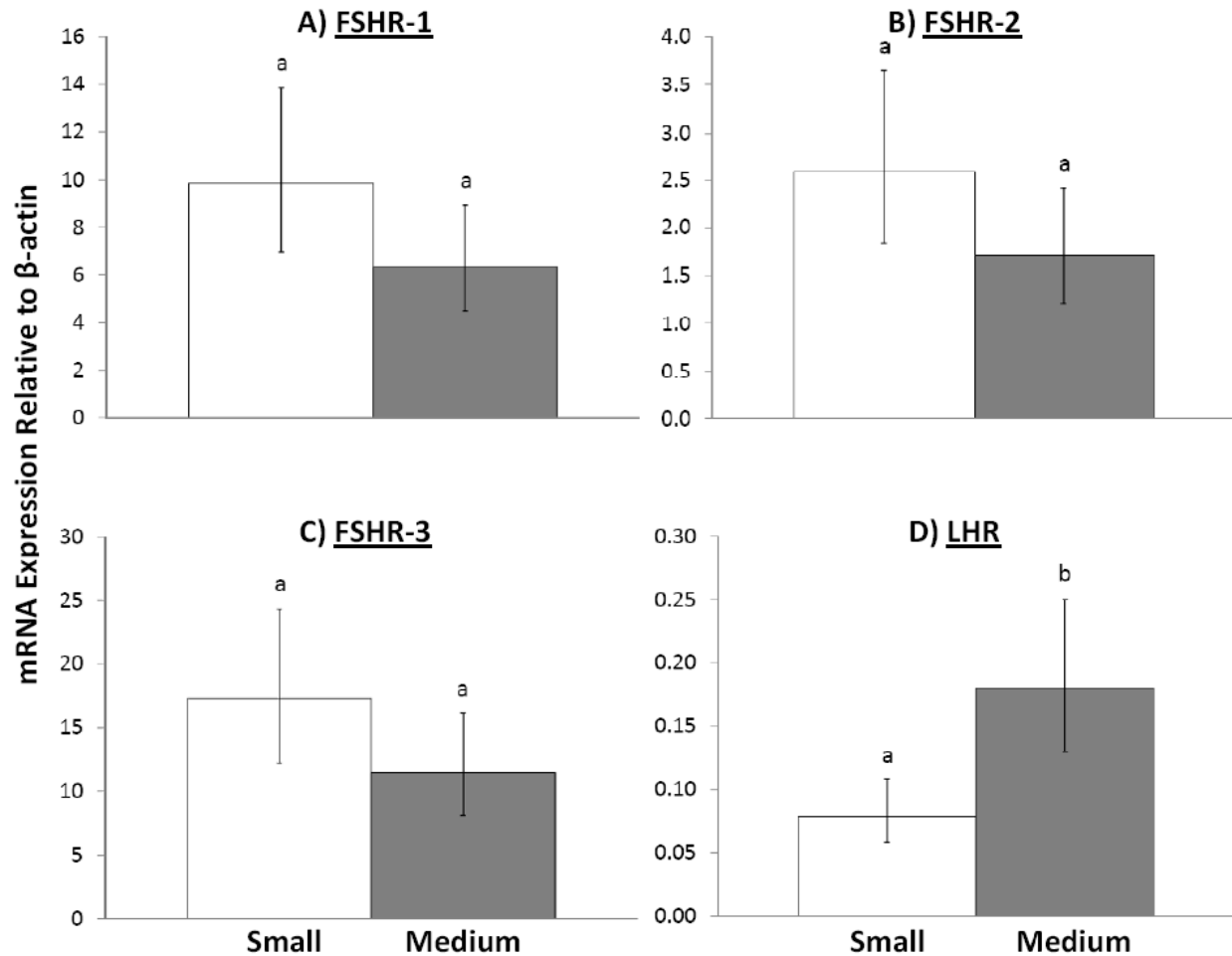


Figure 2.11. Expression of gonadotropin receptors across different sized sheep follicles— Experiment 2.

Granulosa cells were collected from small (≤ 2.0 mm; white bars) and medium (2.1-4.0 mm; gray bars) follicles. After total RNA was extracted, it was subjected to reverse transcription and quantitative PCR. Data are expressed as least squared means of relative expression ($2^{-\Delta Ct} \times 1000$; arbitrary units) \pm SEM. Bars within graphs with differing superscripts are different ($p < 0.05$). Panel A, B, C) Relative expression of FSHR-1, FSHR-2, and FSHR-3 did not differ in small versus medium follicles, although expression was numerically higher in small than medium follicles. Panel D) Relative expression of LHR was higher in medium than small follicles. Overall, LHR expression was the only transcript that differed between small and medium follicles.

When treatment (control versus 500 IU PMSG) and time from CIDR removal to euthanasia (24 versus 36 hours) were compared, no differences in gene expression in different follicles sizes were found (Figures 2.12 and 2.13). Overall, relative expression of FSHR-3 was numerically (but not statistically) higher than other transcripts, regardless of time, treatment, or

follicle size (in the only available comparisons that could be made: small versus medium follicles).

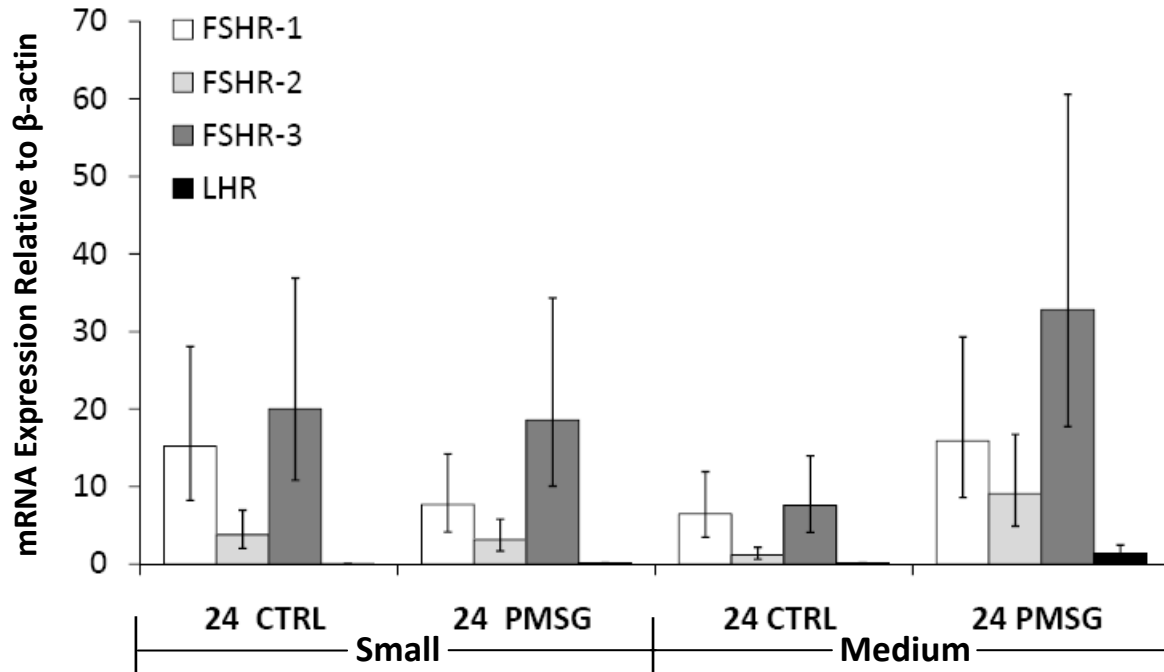


Figure 2.12. Expression of gonadotropin receptors at 24 hours after CIDR removal within small and medium sheep follicles—Experiment 2.

All ewes were treated with CIDRs for 14 days. At CIDR removal, ewes received either no treatment (n=2 control; 24 CTRL), or 500 IU PMSG (n=2; 24 PMSG) and were euthanized 24 hours later. Granulosa cells were collected from small (≤ 2.0 mm) and medium (2.1-4.0 mm) follicles. After total RNA was extracted, it was subjected to reverse transcription and quantitative PCR. Data are expressed as least squared means of relative expression ($2^{-\Delta Ct} \times 1000$; arbitrary units) \pm SEM. Expression of FSHR-1, FSHR-2, FSHR-3 and *LHR* are compared between treatments within a follicle size class. Relative expression of FSHR-3 was numerically higher than other transcripts, but was not statistically different.

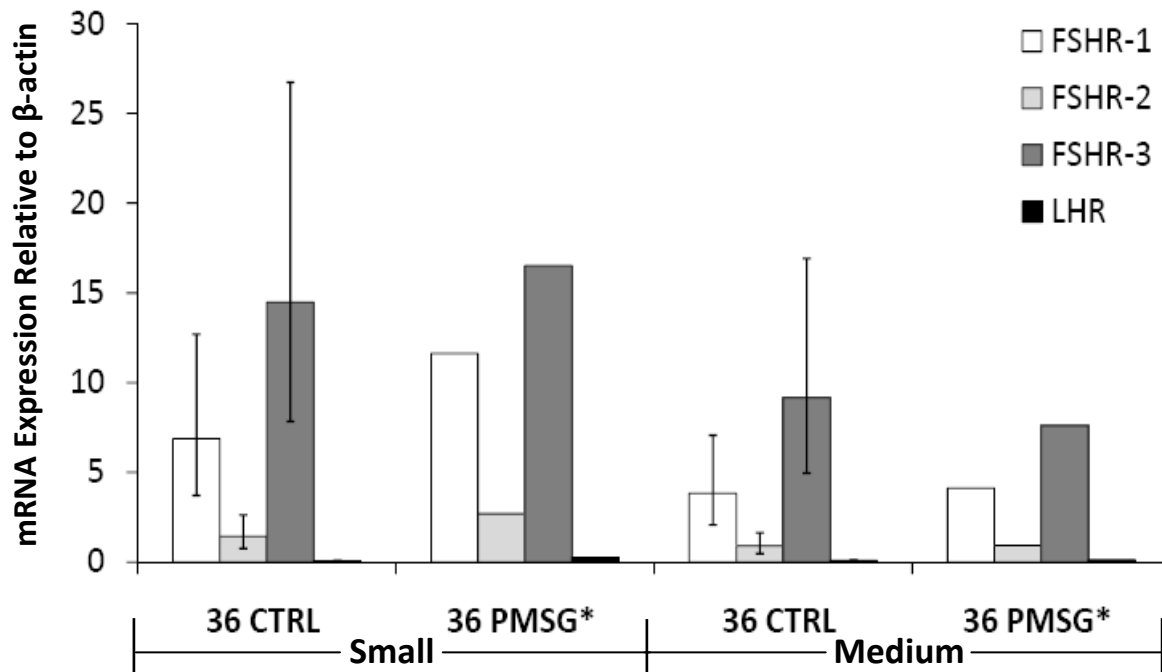


Figure 2.13. Expression of gonadotropin receptors at 36 hours after CIDR removal within small and medium sheep follicles—Experiment 2.

All ewes were treated with CIDRs for 14 days. At CIDR removal, ewes either received no treatment (n=2 control; 36 CTRL), or 500 IU PMSG (36 PMSG*; *relative expression values from one ewe) and were euthanized 36 hours later. Granulosa cells were collected from small (≤ 2.0 mm) and medium (2.1-4.0 mm) follicles. After total RNA was extracted, it was subjected to reverse transcription and quantitative PCR. Data are expressed as least squared means of relative expression ($2^{-\Delta C_t} \times 1000$; arbitrary units) \pm SEM. Expression of FSHR-1, FSHR-2, FSHR-3 and *LHR* are compared between treatments within a follicle size class. Relative expression of FSHR-3 was numerically higher than other transcripts, but was not statistically different.

When large follicle gene expression was evaluated, only raw data could be reported due to sample numbers. Relative expression of *LHR* appeared to increase in small compared to medium follicles (Figure 2.14). Expression of FSHR-2 was numerically lower than both FSHR-1 and FSHR-3.

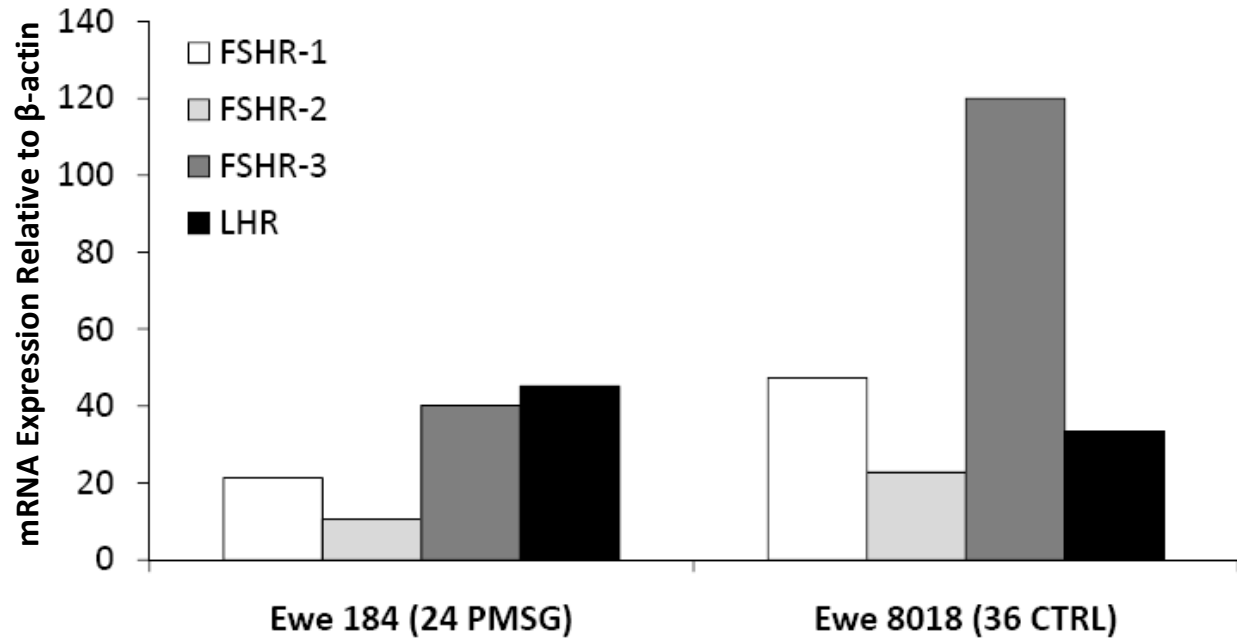


Figure 2.14. Expression of gonadotropin receptors within large sheep follicles— Experiment 2.

All ewes were treated with CIDRs for 14 days. At CIDR removal, ewes received either no treatment or 500 IU PMSG and were euthanized 24 or 36 hours later. Granulosa cells were collected from large (4.1-6.0 mm; only found in two ewes) follicles. After total RNA was extracted, it was subjected to reverse transcription and quantitative PCR. Because only two ewes had follicles of the large class, no statistical analysis could be performed on this size. Data are presented as means (of duplicate wells) of relative expression ($2^{-\Delta Ct} \times 1000$; arbitrary units). Relative expression of FSHR-3 appeared to be higher than other transcripts in Ewe 8018. As with Experiment 1, *LHR* expression appeared to increase with increasing follicle size.

Overall, relative expression of FSHR-2 remained lower than FSHR-1 or FSHR-3 in both experiments. Generally, FSHR-3 expression was numerically higher than other variants, but statistically similar to expression of FSHR-1. Relative expression of *LHR* was low in small and medium follicles, but increased in both large and preovulatory follicles.

Follicular fluid estrogen and progesterone concentrations were determined using RIA. For Experiment 1, estradiol concentrations were consistently lower than progesterone (Figure 2.15); consequently, only one estradiol to progesterone ratio exceeded 1.0. That sample, (Ewe 4, 48 hour; n=3 medium follicles) had ratio of 2.0, and could therefore be considered a pool of healthy follicles.

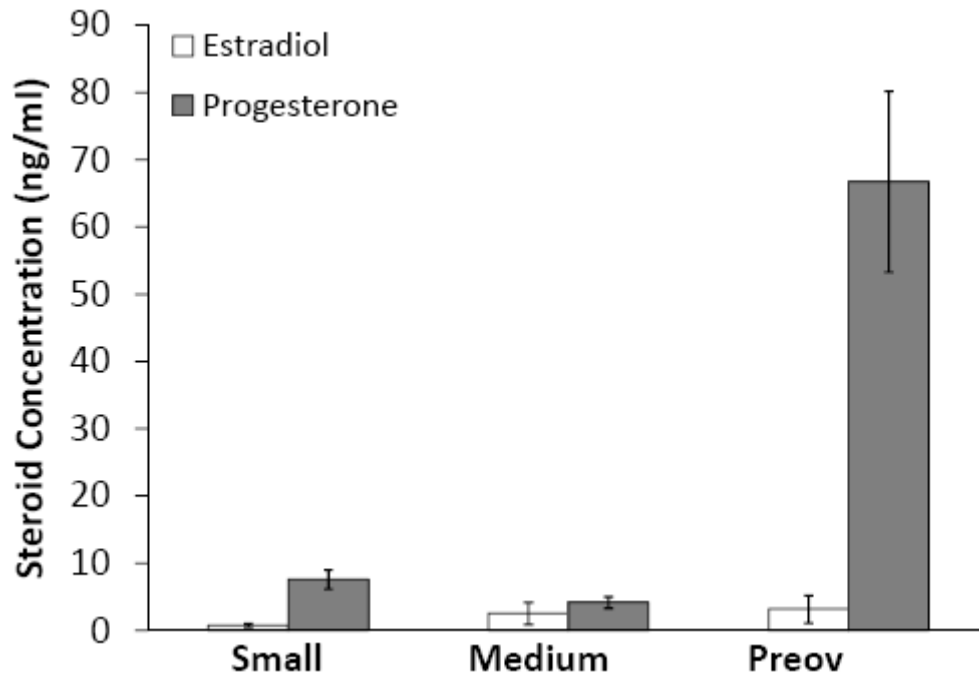


Figure 2.15. Estradiol and progesterone concentrations in follicular fluid from different-sized sheep follicles—Experiment 1.

Follicular fluid was pooled according to follicle diameter: small (≤ 2.0 mm), medium (2.1-4.0 mm) and preovulatory (preov; ≥ 6.1 mm). After granulosa cells were separated by centrifugation, duplicate aliquots (200 μ l total volume) of follicular fluid were analyzed by RIA without extraction. Progesterone concentrations were consistently higher than estradiol in small, medium and preovulatory follicular fluid pools. Data are expressed as mean \pm SEM.

Estradiol concentrations from small follicle pools averaged 0.77 ng/ml. In small follicle pools, follicular fluid from Ewe 11 (36 hour; n=14 follicles) had the lowest (0.07 ng/ml) estradiol concentration while Ewe 16 (24 hour; n=3 follicles) had the highest (2.26 ng/ml) estradiol concentration. Estradiol concentrations for medium follicles averaged 2.53 ng/ml. In medium follicle pools, follicular fluid from Ewe 6 (24 hour; n=7 follicles) had the lowest (0.05 ng/ml) estradiol concentration, while Ewe 4 (48 hour; n=3 follicles) had the highest (13.60 ng/ml) concentration. Estradiol in preovulatory follicles averaged 3.18 ng/ml. Preovulatory follicles were only present in the 24 hour group, with Ewe 12 (24 hour; n=2 follicles) having the lowest (0.91 ng/ml) estradiol concentration and Ewe 16 (24 hour; n=2 follicles) having the highest (7.28 ng/ml) concentration. Mean progesterone concentration in small follicles was 7.61 ng/ml and

ranged from 1.61-10.97 ng/ml. Progesterone concentration in medium follicles averaged 4.18 ng/ml and ranged from 1.38-7.21 ng/ml. Preovulatory follicles had the highest mean progesterone concentration at 66.74 ng/ml, ranging from 43.70-90.29 ng/ml.

The E:P ratio was compared to relative gene expression of each transcript. Correlation values for Experiment 1 are presented in Figure 2.16. Correlation between E:P and expression was the highest for FSHR-2 in small follicles (R=0.4), although FSHR-2 was still the least expressed transcript. In medium follicles, the highest correlation was between E:P and *LHR* (R=0.51).

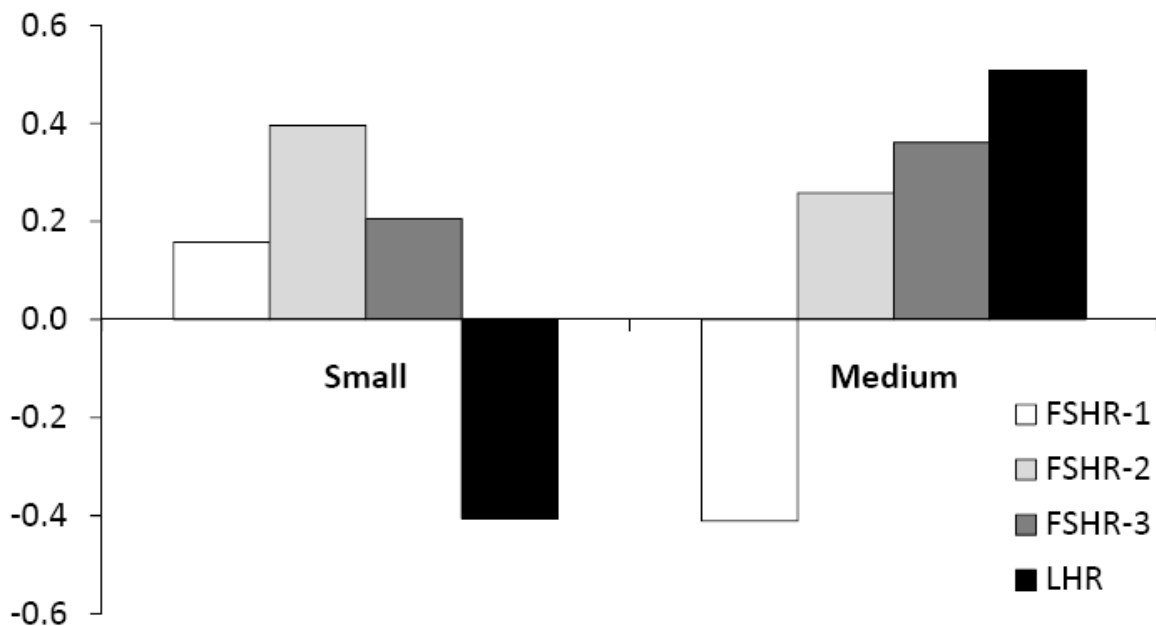


Figure 2.16. Correlation between estradiol to progesterone ratio and gene expression in small and medium sheep follicles—Experiment 1.

Follicular fluid was pooled according to follicle diameter: small (≤ 2.0 mm) and medium (2.1-4.0 mm). After granulosa cells were separated by centrifugation, duplicate aliquots (200 μ l total volume) of follicular fluid were analyzed by RIA without extraction. Estradiol and progesterone concentrations were determined for each sample, and the ratio of estradiol to progesterone was calculated. The FSHR-2 variant had the highest correlation (R=0.4) to the E:P ratio compared to other *FSHR* variants. The E:P was inversely correlated to *LHR* expression in small follicles (R=-0.41), and FSHR-1 expression in medium follicles (R=-0.41). Overall, correlation between E:P and gene expression was low for Experiment 1. Data are expressed as correlation (R) values.

For Experiment 2, follicular fluid estradiol concentrations were lower, on average, than progesterone in small and medium follicles, but higher than progesterone in large follicles (Figure 2.17).

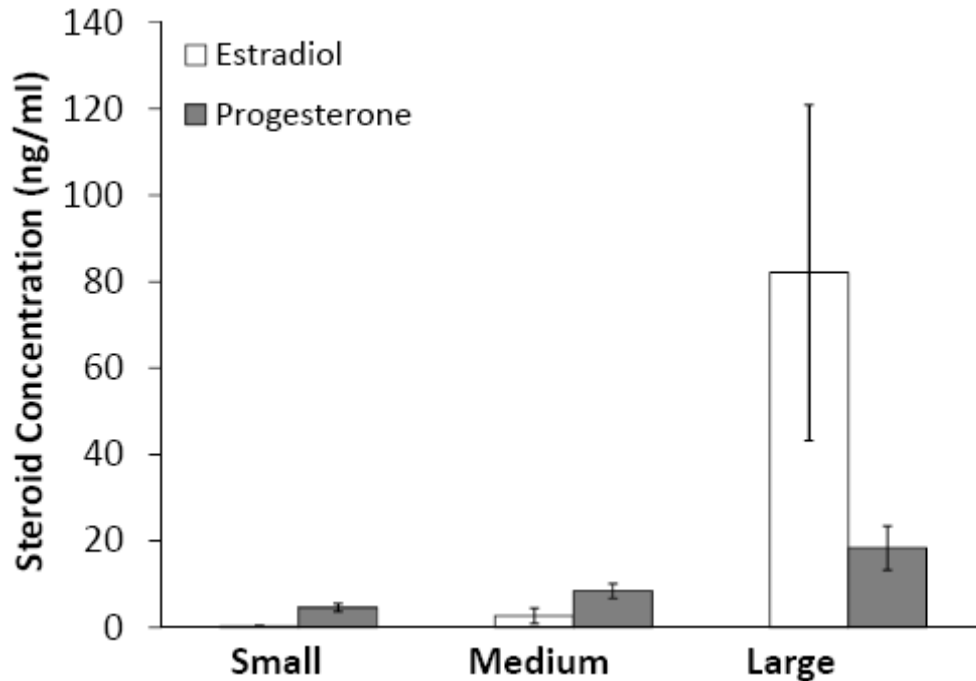


Figure 2.17. Estradiol and progesterone concentrations in follicular fluid from different-sized sheep follicles—Experiment 2.

Follicular fluid was pooled according to follicle diameter: small (≤ 2.0 mm), medium (2.1-4.0 mm) and large (4.1-6.0 mm). After granulosa cells were separated by centrifugation, duplicate aliquots (200 μ l total volume) of follicular fluid were analyzed by RIA without extraction. Progesterone concentrations were higher than estradiol in small and medium, but not large follicular fluid pools. Data are expressed as mean \pm SEM.

Estradiol concentrations for small follicles averaged 0.29 ng/ml; Ewe 8018 (36h control; n=15 follicles) had the lowest (0.108 ng/ml) estradiol concentration while Ewe 8024 (24h control; n=12 follicles) had the highest (0.73 ng/ml) estradiol concentration of small follicle pools. Estradiol concentrations for medium follicles averaged 2.73 ng/ml; Ewe 2 (36h PMSG; n=11 follicles) had the lowest (0.05 ng/ml) estradiol concentration, while Ewe 8076 (24h PMSG; n=8 follicles) had the highest (11.53 ng/ml) concentration of medium follicle pools. Large follicles were present in two ewes: Ewe 184 (24h PMSG; n=2 follicles) and Ewe 8018 (36h

control; n=1 follicle). Estradiol concentration for large follicles collected from Ewe 8018 was 43.26 ng/ml and 120.93 ng/ml for Ewe 184. Mean progesterone concentration in small follicles was 4.59 ng/ml and ranged from 1.37-8.14 ng/ml. Progesterone concentration in medium follicles averaged 8.44 ng/ml and ranged from 4.36-15.63 ng/ml. Large follicles had the highest mean progesterone concentration at 18.38 ng/ml, ranging from 13.27-23.49 ng/ml. Overall, Experiment 2 had more pools with a higher proportion of healthy follicles (as determined by estradiol to progesterone ratio) than Experiment 1.

Correlation between the estradiol to progesterone ratio was higher for Experiment 2 than Experiment 1 (Figure 2.18).

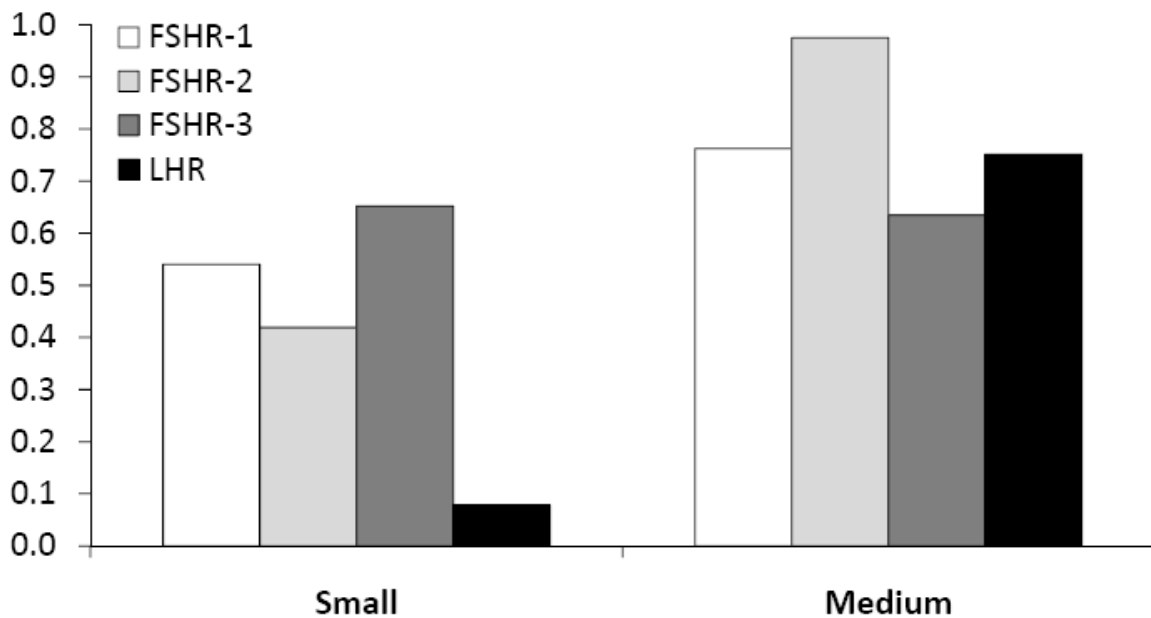


Figure 2.18. Correlation between estradiol to progesterone ratio and gene expression in small and medium sheep follicles—Experiment 2.

Follicular fluid was pooled according to follicle diameter: small (≤ 2.0 mm), medium (2.1-4.0 mm). After granulosa cells were separated by centrifugation, duplicate aliquots (200 μ l total volume) of follicular fluid were analyzed by RIA without extraction. Estradiol and progesterone concentrations were determined for each sample, and the ratio of estradiol to progesterone was calculated. FSHR-2 had the highest correlation ($R=0.98$) to the E:P ratio in medium follicles. Correlation between E:P and *LHR* increased greatly in medium versus small follicles. Overall, the correlation between E:P and gene expression was higher for Experiment 2 than Experiment 1. Data are expressed as correlation (*R*) values.

Correlation between E:P and gene expression in medium follicles was higher than in small follicles. The *LHR* expression was correlated to E:P in medium follicles ($R=0.75$), but not in small follicles ($R=0.08$). In small follicles, correlation between FSHR-3 and E:P was higher ($R=0.65$) than FSHR-1 ($R=0.54$) or FSHR-2 ($R=0.42$). In medium follicles, correlation between FSHR-2 and E:P was higher ($R=0.98$) than FSHR-1 ($R=0.76$) or FSHR-3 ($R=0.64$), even though FSHR-2 was the least expressed transcript.

Serum progesterone concentrations were also determined using RIA. For Experiment 1, serum progesterone values ranged from 0.35-0.67 ng/ml (Table 2.2). For Experiment 2, serum progesterone concentrations immediately prior to CIDR insertion ranged from 0.38-2.69 ng/ml. Serum progesterone concentrations just prior to euthanasia for the same ewes ranged from 0.40-0.64 ng/ml.

Estrous cycle length of ewes in Experiment 1 was similar (Table 2.2) except for one ewe: Ewe 4 exhibited shorter cycles that averaged 8.25 days. Relative expression of FSHR variants within samples collected from Ewe 4 fell in the range of ewes with normal cycle length. As such, those results were included. The average number of follicles found per group for Experiment 1 and 2 are listed in Table 2.2.

Follicle totals for Experiment 1 were as follows: small (≤ 2.0 mm; $n=109$ total; $n=8$ pools), medium (2.1 – 4.0 mm; $n=54$ total; $n=8$ pools) large (4.1-6.0 mm; $n=1$) and preovulatory (≥ 6.1 mm; $n=7$ total; $n=3$ pools). No large follicles were analyzed for RNA expression in Experiment 1 due to sampling errors and/or lack of GC recovery during aspiration. No significant differences were found between collection times (24, 36, or 48 hours after onset of estrus) for number of follicles within a size class.

Group	Time to Euthanasia (hours)	Mean Cycle Length (days)	Number of Follicles				Luteal Tissue (#)			Serum Progesterone	
			≤ 2 mm	2.1-4 mm	4.1-6 mm	≥ 6.1 mm	CH	CL	CA	(ng/ml) ^a	(ng/ml) ^b
Exp 1											
24	22.83 ± 0.24	16.31 ± 0.48	11 ± 8.3	5.7 ± 0.7	0	2 ± 0	0	0.3 ± 0.3	2.0 ± 0.6	n/a	0.43 ± 0.06
36	36.64 ± 0.83	16.80 ± 0.28	15.7 ± 5.0	8.3 ± 2.7	0.3 ± 0.3	0.3 ± 0.3	1.6 ± 0.3	1.0 ± 0.6	2.0 ± 0.6	n/a	0.54 ± 0.14
48	49.33 ± 2.16	13.10 ± 4.85	14.5 ± 2.5	6.0 ± 3.0	0.5 ± 0.5	0	2.5 ± 0.5	1.5 ± 1.5	1.5 ± 0.5	n/a	0.55 ± 0.13
Exp 2											
24 CTRL	24.43 ± 0.05	n/a	17.5 ± 5.5	7.5 ± 0.5	0	0	1.0 ± 0	0.5 ± 0.5	0.5 ± 0.5	0.73 ± 0.31	0.46 ± 0.03
24 PMSG	24.42 ± 0.09	n/a	19.5 ± 2.5	7.0 ± 1.0	1.0 ± 1.0	0	0	0.5 ± 0.5	0.5 ± 0.5	1.65 ± 1.05	0.57 ± 0.07
36 CTRL	36.95 ± 0.02	n/a	18.0 ± 3.0	11.5 ± 5.5	0.5 ± 0.5	0	0.5 ± 0.5	0	0	0.45 ± 0	0.44 ± 0.04
36 PMSG	35.93	n/a	18	11	0	0	1	0	0	0.38	0.44

Table 2.2. Average values for sample collection parameters in Experiment 1 and 2.

For Experiment 1, ewes were monitored through three estrous cycles then euthanized 24, 36, or 48 hours after the onset of the next estrus. For Experiment 2, ewes were euthanized 24 or 36 hours after CIDR removal. Data are presented as means ± SEM. Ovarian structures were measured on the external surface of the ovary with a transparent ruler (to the nearest 0.5mm) and recorded. All visible follicles were aspirated and follicular fluid from each pair of ovaries was pooled according to follicular diameter: small (≤ 2.0 mm), medium (2.1-4.0 mm), large (4.1-6.0 mm) and preovulatory (≥ 6.1 mm). ^aBlood was collected prior to CIDR insertion (for Experiment 2). ^bBlood was collected immediately prior to euthanasia (Experiment 1 and 2).

Follicle totals for Experiment 2 were as follows: small (≤ 2.0 mm; n=95 total; n=7 pools), medium (2.1 – 4.0 mm; n=63 total; n=7 pools), large (4.1-6.0 mm; n=3 total; n=2 pools), and preovulatory (≥ 6.1 mm; n=0). No significant differences were found between collection times (24 or 36 hours after CIDR removal) or treatment group (control vs. PMSG) when comparing numbers of follicles within a size class.

Discussion

In Experiment 1, we have shown that in untreated mature ewes allowed to cycle naturally, the relative expression of FSHR-3 was statistically greater than FSHR-1 in granulosa cells from medium (2.1-4.0 mm) follicles and tended to be higher in small follicles. These results provide the first evidence that FSHR-3 is not a rare transcript in sheep, which is surprising in light of the large number of reports on the G protein-coupled form of the FSH

receptor (FSHR-1). Based on its structure, the FSHR-3 variant has been described to function as a growth factor type-I receptor for FSH [52], thus FSHR-3 could stimulate proliferation of granulosa cells in growing follicles within the ovine ovary. Regardless of follicle size, FSHR-3 expression appeared to exceed that of FSHR-1, indicating that FSHR-3 may be much more important during follicular development than previously thought.

In Experiment 2, *FSHR* variant expression profiles changed after progesterone treatment. Relative expression of *FSHR* variants was numerically higher in small (≤ 2.0 mm) than in medium follicles, which was opposite of that from Experiment 1. This trend was present regardless of treatment or time (24 or 36 hours after CIDR removal) of tissue collection except for *LHR* expression, which was still higher in medium follicles. Expression of *LHR* was expected to increase with increasing granulosa cell differentiation (and follicle diameter) [65-67] and this pattern was observed for both experiments.

For both experiments, FSHR-1 appeared to be expressed in follicles of all sizes at 24, 36, and 48 hours after the onset of estrus or 24 and 36 hours after PMSG treatment. These results agree with Tisdall et al (1995) who found *FSHR* to be expressed in follicles as small as the primary stage, with expression continuing thereafter, even in follicles beginning to undergo atresia [13]. However, Abdennebi et al. and many others have attempted to assess *FSHR* expression using primers or probes that would not discriminate between the different *FSHR* variants [65]. In the current study, care was taken to design primers such that specific variants of the *FSHR* would be discernable.

Relative expression of FSHR-1 was the highest in large follicles following progesterone treatment, and lowest in preovulatory follicles in untreated ewes. Relative expression of FSHR-2

was the lowest of *FSHR* variants, with expression only exceeding (although not significantly) that of *FSHR*-1 in preovulatory follicles.

Other studies have been conducted that examined *FSHR* variant expression in both sheep and mice using RT-PCR and Western blotting. In one study, immature mice (21d) were PMSG-primed (5 IU) and ovaries were harvested 24 or 48 hours later [68]. A two-fold increase was seen in *FSHR*-3 expression over *FSHR*-1 in PMSG-primed mice; a corresponding increase in each receptor protein expression was also observed. We did not see an increase in *FSHR* variant mRNA expression when ewes were hormone-primed with 500 IU PMSG; however, this dose of PMSG was chosen based on protocols (EAZI-BREED™ CIDR®, Pfizer New Zealand, Mt. Eden, Auckland) designed to stimulate out-of-season breeding. McNatty et al. (1982) showed that PMSG (500 IU) priming can decrease atresia of small antral follicles during luteolysis in sheep [69]. McNatty et al. also saw that at 24 hours, the proportion of healthy and atretic follicles was restored to pretreatment levels. Thus, because the effects of PMSG are relatively short-lived, sampling at 12 hours should be considered in the future. In addition, dose-response experiments using PMSG in conjunction with measurement of *FSHR* variant expression would need to be performed before conclusions can be made as to whether PMSG stimulates *FSHR* variant expression in sheep.

To help determine the health of follicles collected in these experiments, progesterone and estradiol concentrations for follicular pools were examined. Steroid content of follicular fluid can be used as an indicator of follicular health status when looking at steroid profiles of individual follicles [70]. In the current study, follicles were pooled for each pair of ovaries based on size criteria, and accordingly, follicular health assessments based on estradiol and progesterone represented “average” follicle health and not actual health of each follicle in which

FSHR variants were measured. Nevertheless, “average” follicle health may provide an initial indication of average *FSHR* variant expression based on stage of development. Expression of *FSHR* variants in Experiment 2 were positively correlated with the estradiol to progesterone ratio in both small and medium follicles.

Because follicles of similar sizes can have very different steroid profiles [38], assessing follicular health based on steroid content can be difficult. Results for Experiment 1 were similar to those of Somchit et al.(2007), in that they observed higher progesterone than estradiol concentrations in pooled follicular fluid from follicles < 3.5 and ≥ 3.5 mm in diameter [71]. We saw the same trend in pools of fluid from small (≤ 2.0 mm) or medium (2.1-4.0mm) follicles [29]. Because progesterone concentrations were consistently higher than estradiol, we believe that a greater number of atretic small or medium follicles were collected than healthy (growing) small or medium follicles. This is a reasonable assumption when considering the mechanism of follicular dynamics. Once follicles reach the preovulatory size, estradiol is no longer the primary hormone produced by the follicle [70], so parameters in addition to the E:P ratio are necessary when assessing follicular health of that follicle size class.

For Experiment 2, more pools of follicles were producing higher levels of estradiol. This could be due to progesterone treatment, or because of PMSG treatment. McNatty et al. (1982) found that after PMSG priming a greater proportion of large antral follicles were producing higher concentrations of estradiol than in control animals [69]. Our results echo this finding, because large (4.1-6.0 mm) follicles produced a higher amount of estradiol than smaller follicles.

Serum progesterone was measured to help assess cycling status. Circulating progesterone concentrations during the luteal phase of ewes are about 3 ng/ml, while progesterone concentrations during estrus are generally less than 1ng/ml [30, 72]. For Experiment 1,

progesterone concentrations collected just prior to euthanasia were under 1ng/ml, so any corpora lutea observed when ovaries were examined after harvest were probably regressing. Low serum progesterone concentrations, taken together with estrus behavior observations, provide compelling evidence that detection of onset of estrus was accurate. For Experiment 2, serum progesterone concentrations in some ewes prior to CIDR insertion indicated the presence of functional corpora lutea. However, serum progesterone concentrations just prior to euthanasia were under 1 ng/ml; the decline in serum progesterone concentrations shows that corpora lutea that were functioning before CIDR insertion (in some ewes) had regressed, and progesterone treatment/synchronization was successful.

Overall number of follicles recovered from each ewe varied greatly. Treatment with PMSG is thought to have little to no effect on the overall number of follicles > 1 mm in diameter [69]. Our results were consistent with previous findings in this regard.

The diverse actions of FSH on follicles during the estrous cycle are well documented, and include stimulation of differentiation, hormone production, and proliferation of granulosa cells. Some of these actions are mediated by FSHR-1 through activation of adenylate cyclase and production of cAMP. The G protein-coupled form of the receptor can also activate other signaling pathways, including extracellular regulated kinases (ERKs), and mitogen-activated protein kinases (MAPKs) [58]. The identification of the *FSHR* nucleotide sequence [5, 6] made it possible to detect alternatively spliced variants of the *FSHR* [7, 8]. The finding that FSHR-3 is the primary form of the *FSHR* in all follicle sizes examined in these experiments supports the idea that other forms of the *FSHR*, in addition to the well characterized G protein-coupled form, may participate in follicular growth and development during the sheep estrous cycle.

CHAPTER 3 - References

1. Sawyer HR, Smith P, Heath DA, Juengel JL, Wakefield SJ, McNatty KP. Formation of ovarian follicles during fetal development in sheep. *Biology of Reproduction* 2002; 66: 1134-1150.
2. Lundy T, Smith P, O'Connell A, Hudson NL, McNatty KP. Populations of granulosa cells in small follicles of the sheep ovary. *Journal of Reproduction and Fertility* 1999; 115: 251-262.
3. Wayne CM, Fan HY, Cheng XD, Richards JS. Follicle-stimulating hormone induces multiple signaling cascades: Evidence that activation of Rous sarcoma oncogene, RAS, and the epidermal growth factor receptor are critical for granulosa cell differentiation. *Molecular Endocrinology* 2007; 21: 1940-1957.
4. Sairam MR, Babu PS. The tale of follitropin receptor diversity: A recipe for fine tuning gonadal responses? *Molecular and Cellular Endocrinology* 2007; 260: 163-171.
5. Yarney TA, Sairam MR, Khan H, Ravindranath N, Payne S, Seidah NG. Molecular-cloning and expression of the ovine testicular follicle-stimulating-hormone receptor. *Molecular and Cellular Endocrinology* 1993; 93: 219-226.
6. Sprengel R, Braun T, Nikolics K, Segaloff DL, Seeburg PH. The Testicular Receptor for Follicle Stimulating Hormone: Structure and Functional Expression of Cloned cDNA. *Molecular Endocrinology* 1990; 4: 525-530.
7. Khan H, Yarney TA, Sairam MR. Cloning of alternatively spliced messenger-RNA transcripts coding for variants of ovine testicular follitropin receptor lacking the G-protein coupling domains. *Biochemical and Biophysical Research Communications* 1993; 190: 888-894.
8. Sairam MR, Jiang LG, Yarney TA, Khan H. Follitropin signal transduction: Alternative splicing of the FSH receptor gene produces a dominant negative form of receptor which inhibits hormone action. *Biochemical and Biophysical Research Communications* 1996; 226: 717-722.
9. Sairam MR, Jiang LG, Yarney TA, Khan H. Alternative splicing converts the G-protein coupled follitropin receptor gene into a growth factor type I receptor: Implications for pleiotropic actions of the hormone. *Molecular Reproduction and Development* 1997; 48: 471-479.

10. Fair T, Hulshof SCJ, Hyttel P, Greve T, Boland M. Oocyte ultrastructure in bovine primordial to early tertiary follicles. *Anatomy and Embryology* 1997; 195: 327-336.
11. Wandji SA, Srsen V, Voss AK, Eppig JJ, Fortune JE. Initiation in vitro of growth of bovine primordial follicles. *Biology of Reproduction* 1996; 55: 942-948.
12. Fortune JE. The early stages of follicular development: activation of primordial follicles and growth of preantral follicles. *Animal Reproduction Science* 2003; 78: 135-163.
13. Tisdall DJ, Watanabe K, Hudson NL, Smith P, McNatty KP. FSH receptor gene-expression during ovarian follicle development in sheep. *Journal of Molecular Endocrinology* 1995; 15: 273-281.
14. Braw-Tal R, McNatty KP, Smith P, Heath DA, Hudson NL, Phillips DJ, McLeod BJ, Davis GH. Ovaries of ewes homozygous for the X-linked Inverdale gene (*FecXI*) are devoid of secondary and tertiary follicles but contain many abnormal structures. *Biol Reprod* 1993; 49: 895-907.
15. Juengel JL, Hudson NL, Heath DA, Smith P, Reader KL, Lawrence SB, O'Connell AR, Laitinen MPE, Cranfield M, Groome NP, Ritvos O, McNatty KP. Growth Differentiation Factor 9 and Bone Morphogenetic Protein 15 Are Essential for Ovarian Follicular Development in Sheep. *Biol Reprod* 2002; 67: 1777-1789.
16. Hanrahan JP, Gregan SM, Mulsant P, Mullen M, Davis GH, Powell R, Galloway SM. Mutations in the genes for oocyte-derived growth factors GDF9 and BMP15 are associated with both increased ovulation rate and sterility in Cambridge and Belclare sheep (*Ovis aries*). *Biology of Reproduction* 2004; 70: 900-909.
17. Galloway SM, McNatty KP, Cambridge LM, Laitinen MPE, Juengel JL, Jokiranta TS, McLaren RJ, Luiro K, Dodds KG, Montgomery GW, Beattie AE, Davis GH, Ritvos O. Mutations in an oocyte-derived growth factor gene (*BMP15*) cause increased ovulation rate and infertility in a dosage-sensitive manner. *Nature Genetics* 2000; 25: 279-283.
18. McNatty KP, Hudson NL, Whiting L, Reader KL, Lun S, Western A, Heath DA, Smith P, Moore LG, Juengel JL. The Effects of Immunizing Sheep with Different BMP15 or GDF9 Peptide Sequences on Ovarian Follicular Activity and Ovulation Rate. *Biol Reprod* 2007; 76: 552-560.
19. Davis GH, McEwan JC, Fennessy PF, Dodds KG, Farquhar PA. Evidence for the presence of a major gene influencing ovulation rate on the X chromosome of sheep. *Biol Reprod* 1991; 44: 620-624.
20. Logan KA, Juengel JL, McNatty KP. Onset of Steroidogenic Enzyme Gene Expression During Ovarian Follicular Development in Sheep. *Biol Reprod* 2002; 66: 906-916.

21. McNatty KP, Heath DA, Lundy T, Fidler AE, Quirke L, O'Connell A, Smith P, Groome N, Tisdall DJ. Control of early ovarian follicular development. In; 1999. 3-16.
22. Cahill LP, Mauleon P. Influences of season, cycle and breed on follicular-growth rates in sheep. *Journal of Reproduction and Fertility* 1980; 58: 321-328.
23. Dufour J, Cahill LP, Mauleon P. Short-term and long-term effects of hypophysectomy and unilateral ovariectomy on ovarian follicular populations in sheep. *Journal of Reproduction and Fertility* 1979; 57: 301-309.
24. Fortune JE. Bovine theca and granulosa-cells interact to promote androgen production. *Biology of Reproduction* 1986; 35: 292-299.
25. Rajakoski E. The ovarian follicular system in sexually mature heifers with special reference to seasonal, cyclical, and left-right variations. *Acta Endocrinologica* 1960; 34: 7-68.
26. Pierson RA, Ginther OJ. Ultrasonic-imaging of the ovaries and uterus in cattle. *Theriogenology* 1988; 29: 21-37.
27. Fortune JE. Ovarian follicular growth and development in mammals. *Biol Reprod* 1994; 50: 225-232.
28. Smeaton TC, Robertso.Ha. Studies on growth and atresia of Graafian follicles in ovary of sheep. *Journal of Reproduction and Fertility* 1971; 25: 243-&.
29. Brand A, Jong W. Qualitative and quantitative micromorphological investigations of tertiary follicle population during estrous-cycle in sheep. *Journal of Reproduction and Fertility* 1973; 33: 431-&.
30. Schrick FN, Surface RA, Pritchard JY, Dailey RA, Townsend EC, Inskeep EK. Ovarian structures during the estrous-cycle and early-pregnancy in ewes. *Biology of Reproduction* 1993; 49: 1133-1140.
31. Evans ACO, Duffy P, Hynes N, Boland MP. Waves of follicle development during the estrous cycle in sheep. *Theriogenology* 2000; 53: 699-715.
32. Driancourt MA, Gibson WR, Cahill LP. Follicular dynamics throughout the estrous-cycle in sheep - a review. *Reproduction Nutrition Development* 1985; 25: 1-15.
33. Turnbull KE, Braden AWH, Mattner PE. Pattern of follicular-growth and atresia in ovine ovary. *Australian Journal of Biological Sciences* 1977; 30: 229-241.
34. Adams GP, Matteri RL, Kastelic JP, Ko JCH, Ginther OJ. Association between surges of follicle-stimulating-hormone and the emergence of follicular waves in heifers. *Journal of Reproduction and Fertility* 1992; 94: 177-188.

35. Evans ACO, Flynn JD, Duffy P, Knight PG, Boland MP. Effects of ovarian follicle ablation on FSH, oestradiol and inhibin A concentrations and growth of other follicles in sheep. *Reproduction* 2002; 123: 59-66.
36. Beg MA, Bergfelt DR, Kot K, Ginther OJ. Follicle selection in cattle: Dynamics of follicular fluid factors during development of follicle dominance. *Biology of Reproduction* 2002; 66: 120-126.
37. Caraty A, Locatelli A, Martin GB. Biphasic response in the secretion of gonadotropin-releasing hormone in ovariectomized ewes injected with estradiol. *Journal of Endocrinology* 1989; 123: 375-382.
38. Carson RS, Findlay JK, Clarke IJ, Burger HG. Estradiol, testosterone, and androstenedione in ovine follicular-fluid during growth and atresia of ovarian follicles. *Biology of Reproduction* 1981; 24: 105-113.
39. Stanton PG, Burgon PG, Hearn MTW, Robertson DM. Structural and functional characterisation of hFSH and hLH isoforms. *Molecular and Cellular Endocrinology* 1996; 125: 133-141.
40. Ulloa-Aguirre A, Timossi C, Damian-Matsumura P, Dias JA. Role of glycosylation in function of follicle-stimulating hormone. *Endocrine* 1999; 11: 205-215.
41. Ferris HA, Shupnik MA. Mechanisms for pulsatile regulation of the gonadotropin subunit genes by GNRH1. *Biology of Reproduction* 2006; 74: 993-998.
42. Bilezikjian LM, Blount AL, Leal AMO, Donaldson CJ, Fischer WH, Vale WW. Autocrine/paracrine regulation of pituitary function by activin, inhibin and follistatin. *Molecular and Cellular Endocrinology* 2004; 225: 29-36.
43. Sairam MR, Subbarayan VSR. Characterization of the 5' flanking region and potential control elements of the ovine follitropin receptor gene. *Molecular Reproduction and Development* 1997; 48: 480-487.
44. Xing WR, Sairam MR. Characterization of regulatory elements of ovine follicle-stimulating hormone (FSH) receptor gene: The role of E-box in the regulation of ovine FSH receptor expression. *Biology of Reproduction* 2001; 64: 579-589.
45. Findlay JK, Drummond AE. Regulation of the FSH receptor in the ovary. *Trends in Endocrinology and Metabolism* 1999; 10: 183-188.
46. Ulloa-Aguirre A, Uribe A, Zarinan T, Bustos-Jaimes I, Perez-Solis MA, Dias JA. Role of the intracellular domains of the human FSH receptor in G(alpha S) protein coupling and receptor expression. *Molecular and Cellular Endocrinology* 2007; 260: 153-162.

47. Alberts B, Johnson A, Lewis J, Raff M, Roberts K, Walter P. Molecular Biology of the Cell. In: Gibbs S (ed.), 2002 ed. New York: Garland Science; 2002.
48. Solis AS, Shariat N, Patton JG. Splicing fidelity, enhancers, and disease. *Frontiers in Bioscience* 2008; 13: 1926-1942.
49. Sharp PA. The discovery of split genes and RNA splicing. *Trends in Biochemical Sciences* 2005; 30: 279-281.
50. Yarney TA, Jiang LG, Khan H, MacDonald EA, Laird DW, Sairam MR. Molecular cloning, structure, and expression of a testicular follitropin receptor with selective alteration in the carboxy terminus that affects signaling function. *Molecular Reproduction and Development* 1997; 48: 458-470.
51. Touyz RM, Jiang LG, Sairam MR. Follicle-stimulating hormone mediated calcium signaling by the alternatively spliced growth factor type I receptor. *Biology of Reproduction* 2000; 62: 1067-1074.
52. Babu PS, Krishnamurthy H, Chedrese PJ, Sairam MR. Activation of extracellular-regulated kinase pathways in ovarian granulosa cells by the novel growth factor type 1 follicle-stimulating hormone receptor - Role in hormone signaling and cell proliferation. *Journal of Biological Chemistry* 2000; 275: 27615-27626.
53. Bittman EL, Dempsey RJ, Karsch FJ. Pineal melatonin secretion drives the reproductive response to daylength in the ewe. *Endocrinology* 1983; 113: 2276-2283.
54. Bittman EL, Karsch FJ. Nightly duration of pineal melatonin secretion determines the reproductive response to inhibitory day length in the ewe. *Biology of Reproduction* 1984; 30: 585-593.
55. Malpaux B, Robinson JE, Brown MB, Karsch FJ. Importance of changing photoperiod and melatonin secretory pattern in determining the length of the breeding-season in the suffolk ewe. *Journal of Reproduction and Fertility* 1988; 83: 461-470.
56. Rosa HJD, Bryant MJ. Seasonality of reproduction in sheep. *Small Ruminant Research* 2003; 48: 155-171.
57. Bartlewski PM, Beard AP, Rawlings NC. Ovarian function in ewes during the transition from breeding season to anoestrus. *Animal Reproduction Science* 1999; 57: 51-66.
58. Hunzicker-Dunn M, Maizels ET. FSH signaling pathways in immature granulosa cells that regulate target gene expression: Branching out from protein kinase A. *Cellular Signalling* 2006; 18: 1351-1359.
59. Ulloa-Aguirre A, Zarina T, Pasapera AM, Casas-Gonzalez P, Dias JA. Multiple facets of follicle-stimulating hormone receptor function. *Endocrine* 2007; 32: 251-263.

60. Keller-Rhodes AE, Grieger DM, Rozell TG. Stage specific expression of follicle stimulating hormone receptor variants during bovine folliculogenesis. In; 2004. 295.
61. Rozell TG, Monteiro AM, Baker PJ, Mihm M. Evidence for differential expression of FSH receptor exons 10 and 11 during follicular wave development in the cow. *Biology of Reproduction* 2005; 179-179.
62. Skaggs CL, Able BV, Stevenson JS. Pulsatile or Continuous Infusion of Luteinizing Hormone-Releasing Hormone and Hormonal Concentrations in Prepubertal Beef Heifers. *J. Anim Sci.* 1986; 62: 1034-1048.
63. Prendiville DJ, Enright WJ, Crowe MA, Finnerty M, Hynes N, Roche JF. Immunization of heifers against gonadotropin-releasing hormone: antibody titers, ovarian function, body growth, and carcass characteristics. *J. Anim Sci.* 1995; 73: 2382-2389.
64. Evans ACO, Ireland JLH, Winn ME, Lonergan P, Smith GW, Coussens PM, Ireland JJ. Identification of genes involved in apoptosis and dominant follicle development during follicular waves in cattle. *Biology of Reproduction* 2004; 70: 1475-1484.
65. Abdennebi L, Monget P, Pisselet C, Remy JJ, Salesse R, Monniaux D. Comparative expression of luteinizing hormone and follicle-stimulating hormone receptors in ovarian follicles from high and low prolific sheep breeds. *Biology of Reproduction* 1999; 60: 845-854.
66. Bao B, Garverick HA, Smith GW, Smith MF, Salfen BE, Youngquist RS. Changes in messenger ribonucleic acid encoding luteinizing hormone receptor, cytochrome P450-side chain cleavage, and aromatase are associated with recruitment and selection of bovine ovarian follicles. *Biol Reprod* 1997; 56: 1158-1168.
67. Webb R, England BG. Identification of the ovulatory follicle in the ewe - associated changes in follicular size, thecal and granulosa-cell luteinizing-hormone receptors, antral fluid steroids, and circulating hormones during the preovulatory period. *Endocrinology* 1982; 110: 873-881.
68. Babu PS, Danilovich N, Sairam MR. Hormone-induced receptor gene splicing: Enhanced expression of the growth factor type I follicle-stimulating hormone receptor motif in the developing mouse ovary as a new paradigm in growth regulation. *Endocrinology* 2001; 142: 381-389.
69. McNatty KP, Gibb M, Dobson C, Ball K, Coster J, Heath D, Thurley DC. Preovulatory follicular development in sheep treated with PMSG and or prostaglandin. *Journal of Reproduction and Fertility* 1982; 65: 111-123.
70. Ireland JJ, Roche JF. Growth and differentiation of large antral follicles after spontaneous luteolysis in heifers - changes in concentration of hormones in follicular-fluid and

specific binding of gonadotropins to follicles. *Journal of Animal Science* 1983; 57: 157-167.

71. Somchit A, Campbell BK, Khalid M, Kendall NR, Scaramuzzi RJ. The effect of short-term nutritional supplementation of ewes with lupin grain (*Lupinus luteus*), during the luteal phase of the estrous cycle on the number of ovarian follicles and the concentrations of hormones and glucose in plasma and follicular fluid. *Theriogenology* 2007; 68: 1037-1046.
72. Senger PL. *Pathways to Pregnancy and Parturition*. Pullman, WA: Current Conceptions, Inc.; 1997.

Appendix A - Protocols and Forms

Aspiration Protocol

- Consider both ovaries from a single ewe one sample.
- Measure (using a transparent ruler, from the outer surface of the ovary) and chart ovarian structures (insert chart).
- Aspirate follicular fluid from each follicle using a 1 cc syringe and a 20 gauge needle.
- To ensure adequate granulosa cells are recovered, insert the needle into a follicle and aspirate the follicular fluid into the syringe and then gently push it back into the same follicle three times before removing the needle and moving to the next follicle.
- Use a new syringe and needle for each ewe and each follicle size class.
- Pool follicular fluid from follicles of similar diameter (small ≤ 2.0 mm; medium 2.1 – 4.0 mm; large 4.1-6.0mm; preovulatory ≥ 6.1 mm) into 1.5 μ l microcentrifuge tubes.
- Place tubes in microcentrifuge.
- Centrifuge 2 minutes at 2300xg.
- Aspirate supernatant and place in clean microcentrifuge tube – freeze in -20°C for E2/P4 assay.
- Cover each cell pellet with 0.5 ml PBS.
- Resuspend by finger-flicking or gentle pipetting.
- Centrifuge 1 minute at 2300xg.
- Aspirate and discard PBS (leave a small amount to avoid disturbing the cell pellet).
- Add 1 ml Trizol to each sample.
- Resuspend the cell pellet by aspirating with a filtered 1 ml pipette tip.
- Freeze in the -20°C (if less than one month) or -80°C (longer than one month) until RNA extraction.

RNA Extraction from Trizol samples

- Trizol contains phenol, thus, it is the first step in a phenol/chloroform RNA extraction.
- Thaw trizol samples (containing cell lysates in 1 ml Trizol) at room temp for 3-5 minutes.
- Mix by inverting (about 10 times/minute) while thawing.
- Go next door to the yellow flammables cabinet and take Chloroform:Isoamylalcohol (24:1) and 2-Propanol (Isopropanol) to the hood. Measure approximately 1 ml of each into two 15 ml conical tubes and leave (capped) in the hood. Place large containers back into the flammables cabinet.
- Take thawed Trizol samples, pipetman, tips, timer, and lab book to the hood.
- Add 200 μ l Chloroform:Isoamylalcohol to each Trizol sample (put excess ChCl_3 into the Hazardous Waste container marked “Chloroform” in the hood).
- Mix vigorously by hand for 15 seconds.
- Incubate 3 minutes at room temperature (mix by hand several times while incubating).
- Take capped samples to the microcentrifuge.
- Place samples inside and ensure that the centrifuge fume cap is on.
- Centrifuge for 15 minutes at full speed.
- Label new tubes while this is spinning.
- Take samples and new tubes back to the hood.
- Aspirate aqueous fraction (clear liquid at the top, being careful to avoid the white protein layer).
- Transfer to new tube – try to get about 500 μ l of aqueous fraction removed/transferred.
- Cap the old tubes and discard the remaining pink phase into the Haz. Waste bag in the hood (if you will be extracting protein or DNA from the samples, keep the pink phase; store it at -80°C until extraction).
- Add 500 μ l Isopropanol to each sample (put excess into the Haz. Waste container marked “2-propanol” in the hood).
- Incubate 10 minutes at room temperature.

- Take capped samples to the microcentrifuge—always spin tubes such that the pellet forms on the hinge side of the microcentrifuge tube to avoid disturbing the pellet whenever it is invisible.
- Centrifuge for 10 minutes at full speed—use fume cap.
- Take samples back to the hood.
- Remove the supernatant liquid and discard – into the “2-propanol” Haz. Waste bag in the hood (you may or may not be able to see an RNA pellet at this point; if no pellet is visible, leave a very thin layer of isopropanol in the bottom of the tube to avoid removing the RNA).
- Add 1mL 75% EtOH (Ethanol and Water) to the precipitate and vortex very gently/briefly.
- Centrifuge for 5 minutes at full speed (again, aligning all tubes the same way).
- Preheat ~500 μ l ddH₂O at 65°C.
- Aspirate EtOH carefully, keeping away from pellet.
- Air dry pellets for 5-10 minutes.
- Be sure all EtOH has evaporated; otherwise, RNA may not resuspend.
- Add 15 μ l preheated ddH₂O and finger-flick to mix.
- Incubate 10 minutes at 65°C.
- Freeze extracted total RNA in the -80°C freezer (RNA is not very stable).

DNase Treat RNA TURBO DNA-free Protocol

- Use 0.5 mL microcentrifuge tubes
- Prepare Master Mix on ice (prepare enough for ½ - 1 extra reaction):

	<u>1 tube</u>	<u>*? tubes</u>
10X Turbo DNase Buffer	1.2 µl	____µl
TURBO DNase	0.5 µl	____µl
ddH ₂ O	<u>2.8 µl</u>	____µl
	4.5 µl	

- Add 4.5 µl master mix to each tube.
- Add 7.5 µl RNA to each tube.
- Incubate 40 minutes at 37°C (can use waterbath).
- Vortex the DNase inactivation reagent.
- Add 4 µl DNase inactivation reagent to each tube and finger flick to mix.
- Incubate 3 minutes at room temp.
- Finger flick several times to disperse the inactivation reagent.
- Centrifuge for 1.5 minutes at 10,000 rpm.
- Carefully transfer the supernatant containing the RNA into a new tube.
- Avoid the inactivation reagent, as it can interfere with downstream reactions.
- Final sample volume should be 10-12 µl.
- Store in the -80°C freezer. DNase treated RNA is unstable.

RT-PCR Protocol - SuperScript III First-Strand Synthesis SuperMix

- Use this kit to convert DNase treated RNA to cDNA.
- Starting material: 10 pg to 1 µg DNase treated (total) RNA
- Combine the following kit components in a .2 ml or .5 ml thin-walled PCR tube on ice. For multiple reactions, a master mix without RNA may be prepared:

	<u>1 rxn</u>	<u>*? rxns</u>
-2X RT Reaction Mix	<u>10 µl</u>	<u>— µ</u>
-RT Enzyme Mix	<u>2 µl</u>	<u>—µl</u>
-RNA (10 pg to 1 µg total RNA)	<u>x µl</u>	<u>—µl</u>
-ddH2O	<u>to 20 µl</u>	<u>—µl</u>
	20 µl	µl

- Gently mix tube contents and incubate at 25°C for 10 minutes.
- Incubate at 42°C for 50 minutes.
- Terminate the reaction at 85°C for 5 minutes.
- Chill on ice.
- Add 1 µl of *E. coli* RNase H and incubate at 37°C for 20 minutes.
- Use 1 µl of undiluted cDNA to prepare template for qPCR or store the reaction at -20°C until use.

Real-Time PCR Protocol - Platinum SYBR Green qPCR SuperMix-UDG with ROX

- For multiple reactions, prepare a master mix of common components.
- Prepare a 96-well plate map with template and primer set information. For example, see table X.
- Label 0.5 ml microcentrifuge tubes with primer set name, template name, or master mix. The following volumes have been scaled down to give a 20µl reaction volume; prepare the following on ice:

Primer mastermixes:

<u>Component</u>	<u>Per reaction</u>	<u>x ? Rxns</u>
Platinum SYBR Green	<u>10 µl</u>	<u>— µl</u>
Forward Primer (250nM)	<u>.25 µl</u>	<u>— µl</u>
Reverse Primer (250nM)	<u>.25 µl</u>	<u>— µl</u>
ddH2O (to 15 µl)	<u>4.5 µl</u>	<u>— µl</u>
	15 µl per well	? µl total

- For each template, prepare a dilution.

<u>cDNA template:</u>	<u>Per well</u>	<u>x ? wells</u>
cDNA template	<u>1 µl</u>	<u>— µl</u>
ddH2O (to 5 µl)	<u>4 µl</u>	<u>— µl</u>
	5 µl per well	? µl total

- Once the primer master mixes and template are prepared, take them (on ice) to Colleen's lab.
- Load a 96-well plate according to the map you have prepared.
- You will add 15 µl primer master mix and 5 µl diluted cDNA template per well for a final reaction volume of 20 µl.

Program the ABI Prism 7500 as follows:

50°C for 2 minutes hold (1 cycle)

95°C for 2 minutes hold (1 cycle)

40 cycles of:

95°C, 15 seconds

60°C, 30 seconds

DNA Gel Protocol

- For a large, 2% agarose gel:
- Use masking tape to seal the two open sides of the large gel cassette
- Find the corresponding comb
- Use 160 ml 1X TBE
 - 160 ml * 0.02 = 3.2 g agarose (in tall cabinet on east wall)
- Combine 160 ml 1X TBE and 3.2 g agarose in a 500 ml Erlenmeyer flask, swirl
- Microwave approximately 1 minute, 10 seconds.
- Swirl
- Microwave about 20 seconds longer, or until it begins to boil
- Swirl
- Cool by running cold tap water on the outside of the beaker, about 1 minute
- Add 0.6 µl EtBr, swirl
- Pour into taped gel cassette with comb in place
- Remove air bubbles with a pipette tip
- Let cool and gel set (about 10 min - while this is cooling, prepare samples)
 - place ~40 µl sample (DNA) and 4.5 µl Ficoll sample buffer in a microcentrifuge tube
 - repeat for each sample
- Remove tape and comb
- Put cooled gel (in cassette) into the large gel box
- Fill with 1X TBE until gel is submerged
- Load samples:
 - Use 6.5 µl (100bp) ladder in lane 1
 - Use 30 µl prepared sample per well
- Run for ~2 hours at 70 volts (run toward red)

Estradiol RIA Protocol

A. DIAGNOSTIC PRODUCTS CORPORATION (DPC) ESTRADIOL DOUBLE ANTIBODY KIT (# KE2D1) WITH MODIFICATIONS

Dilute ovine follicular fluid from small and medium-sized follicles 1:100 in zero calibrator prior to assay. Follicular fluid from large follicles may need dilution at 1:500.

1. Estradiol Antiserum (# E2D1) 1 vial of lyophilized estradiol antiserum, raised in rabbits. Add 10 ml of Milli-Q-water. Store refrigerated: stable at 4°C for 30 days after reconstitution.
3. ¹²⁵I Estradiol (#E2D2) 1 vial of iodinated synthetic Estradiol in liquid form, 11ml, 3.5µCi. Store refrigerated: stable at 4°C for 30 days after opening, or until the expiration date marked on the label.
3. Estradiol Calibrators/Standards (# E2D3-9) One set of seven glass vials, labeled A through G, of Estradiol calibrators, with preservative. The zero calibrator A (also referred to as RIA Buffer or Estradiol Calibrator Matrix) contains 6 ml, and the remaining calibrators B through G contain 3 ml each. Store refrigerated: stable at 4°C for 30 days after opening.
4. Precipitating Solution (# N6), 110 ml. One vial consisting of goat anti-rabbit gamma globulin and dilute PEG in saline. Store refrigerated: stable at 4°C for 30 days after opening.

B. RIA STANDARDS and REAGENTS

1. Assay Standards: Standards come ready for use in the kit. Note: The concentration of unknown samples run in 100 µl volumes will be read off the standard curve at pg/ml values. If sample dilutions are made, the concentration needs to be adjusted.

<u>Standard Vial labeled</u>	<u>Concentration at 100 µl per tube</u>
A. 0 pg/ml (Maximum Binding)	0 pg/ml
B. 5 pg/ml	2.5 pg/ml
C. 10 pg/ml	5 pg/ml
D. 20 pg/ml	10 pg/ml
E. 50 pg/ml	25 pg/ml
F. 150 pg/ml	75 pg/ml
G. 500 pg/ml	250 pg/ml

2. Estradiol Antiserum At least 10 minutes before use, reconstitute vial by adding 10 ml Milli-Q water or bring to room temperature (RT) if stored at 4°C. Mix by gentle inversion.

3. Quality Controls To ensure assay is running properly:

QC1 Use standard C 100 μ l = 5 pg/ml (four tubes – 2 for beginning and end of run)

For Inter-assay controls (CV between assays):

Make the following dilutions using an ovine follicular fluid (oFF) standard:

QC2 1:100 dilution of oFF (495 μ l RIA calibrator matrix + 5 μ l oFF standard (four tubes))

For Intra-assay controls (CV within an assay):

A second set of quality controls can be placed at the end of an assay greater than 200 tubes.

A. RIA PROTOCOL

Note: Rainin pipettes are used for standard and sample preparation. Eppendorf repeater pipette is used for the addition of Estradiol Antiserum, 125I-Estradiol, and Precipitation Solution.

1. Set up:

a. Label 12 x 75 mm polypropylene tubes:

- Total Count (TC, tubes 1 and 2).
- Non-Specific Binding (NSB, tubes 3 and 4)
- Maximum Binding (MB, tubes 5 and 6)
- Standards (tubes 7-18; at least three additional standards can be added to the lower end of the curve, if desired).
- Quality Controls (QC1, tubes 19 and 20; QC2, tubes 21 and 22; QC3, tubes 23 and 24).
- Samples will start at tube 25 and will be run in duplicate.

b. Place tubes in racks on trays covered with lab bench paper.

c. Bring all samples and RIA components, except Precipitating Solution, to RT before use.

d. TC tubes are left empty at this point.

e. To the NSB tubes, add 100 μ l RIA calibrator matrix.

f. To the MB tubes, add 100 μ l RIA calibrator matrix.

g. To the standard tubes (7-18), add 100 μ l of each standard concentration (2.5 to 250 pg/ml, B to G) in ascending order, in duplicate.

h. To QC1, QC2, and QC3, add 100 μ l of the indicated quality control.

i. To tubes 25 and above, add samples. Total volume is 100 μ l. Any dilutions are made in RIA calibrator matrix.

2. Assay

- a. Add 30 μl of Estradiol Antiserum to all tubes except TC and NSB tubes (tubes 1-4).
Vortex and incubate at RT for 2 hours.
- b. Add 75 μl of ^{125}I -Estradiol to all tubes. Cap TC tubes and set aside until counting.
- c. Vortex and incubate at RT for 1 hour.
- d. Write out amount (0.024 $\mu\text{Ci}/\text{tube}$) of radioactivity, date, and initials on Rad tape and place on the covered tray containing the tubes.
- e. Add 1 ml of *cold* Precipitating Solution to all tubes except TC tubes.
Vortex and incubate at RT for 10 minutes.
- f. Centrifuge all tubes, except TC, at 3,100 x g for 15 min at 4°C.
- g. Take tubes (in centrifuge racks) to the radioactive hood. Pour supernatant into metal pan. Keeping tubes inverted, rap sharply on paper towels, then move to dry paper towels. Every 5 minutes for ~ 15 minutes (3 times), rap the inverted tubes sharply on the paper towels and move to dry towels. If no hanging droplets are present, proceed to counter.
- h. Count tubes for 1 min in Gamma Counter.
- i. Dispose liquid in bound ^{125}I radioactive liquid waste carboy (0.02 $\mu\text{Ci}/\text{tube}$) and paper in solid bound ^{125}I radioactive waste can (0.004 $\mu\text{Ci}/\text{tube}$).
- j. Use Assay Zap software and Estradiol.azm method to calculate Estradiol concentration in samples.

D. ADDITIONAL MATERIALS FROM DPC

In addition to reagents supplied in the kit (# KE2D1), additional reagents may be needed depending on the number of samples to be assayed.

1. Estradiol Antiserum (# E2D1) comes lyophilized; add 10 ml Milli-Q-water
2. ^{125}I Estradiol (#E2D2) contains 11 ml, 3.5 μCi
3. Estradiol Calibrator Matrix (#10EDZ) contains 100 ml
4. Precipitating Solution (#5N6), contains 260 ml or (#N6) contains 110 ml

E. REFERENCES

1. Diagnostic Products Corporation. Double Antibody Estradiol RIA protocol.
2. Turzillo, A.M. and Fortune, J. E. 1990. Suppression of the secondary FSH surge with bovine follicular fluid associated with delayed ovarian follicular development in heifers. J. Reprod. Fert. 89:643.
3. Ireland, JLH, Ireland, JJ. 1994. Changes in expression of inhibin/activin α_A and β_B subunit

messenger ribonucleic acids following increases in size and during different stages of differentiation or atresia of non-ovulatory follicles in cows. Biol Reprod 50:492-501.

Progesterone RIA Protocol

Siemens Medical Solutions Diagnostics Progesterone COAT-A-COUNT Assay (#TKPG1)

All components must be at room temperature before use.

Prepare ovine follicular fluid samples prior to assay by diluting 1 µl follicular fluid in 49 µl zero calibrator.

All components must be at room temperature before use.

1. Plain tubes: Label four uncoated 12x75mm polypropylene tubes TC (total counts) and NSB (nonspecific binding) in duplicate.

Coated tubes: Label fourteen Progesterone Ab-coated tubes with standard curve concentrations, starting with 0 ng/ml in duplicate. At least two additional standards can be added to the lower end of the curve, if desired. Label additional Ab-coated tubes, also in duplicate for controls and samples.

2. Pipette 100 µl of the zero calibrator into the NSB and 0 ng/ml tubes, and 100 µl of each of the standard curve calibrators into its designated tubes. Pipette 100 µl of each control and unknown samples into the tubes prepared.

Because progesterone has a tendency to adsorb to plastic, and even more so to glass, it is important to dispense each sample into the very bottom of each tube. In addition, it is also important to coat the pipette tip by rinsing a few times in the sample before making the transfer to the tube. Also, change tips between each standard and sample.

Samples expected to exceed 40 ng/ml should be diluted in the zero calibrator before assay.

3. Add 1.0 ml of ¹²⁵I Progesterone to every tube. Vortex.

No more than ten minutes should elapse during dispensing of the tracer. Set the TC tubes aside for counting; they require no further processing.

4. Incubate for 3 hours at room temperature.
5. Decant thoroughly.

Removing all visible moisture will greatly enhance precision. Using a foam decanting rack, decant the contents of all tubes (except for TC) in the radioactive hood (in an appropriate container) and allow them to drain on paper towels for 2 or 3 minutes. The strike tubes sharply on paper towels to remove residual droplets.

6. Count for 1 minute with gamma counter.

RNA Quality Protocol-Agilent 2100 Bioanalyzer with Agilent 6000 Nano Kit

The Bioanalyzer is located in the COBRE lab in Coles Hall. You must register for an account with Kalidou Ndiaye to use this machine.

Turn on waterbath (heat to 70 C)

Preparing the Gel-Dye Mix

1. Allow the RNA 6000 Nano dye concentrate (blue) to equilibrate to room temperature for 30 minutes.
2. Spin down the dye, filtered gel, and marker for about 30 seconds.
3. Add 65 μ L filtered gel (red) to 1 μ l dye and vortex for about 15 seconds.
4. Centrifuge at 13000xg for 10 minutes at room temperature. Use within one day.

While this is spinning, go upstairs to room 223 and get an aliquot of Nano ladder from the freezer. Place on ice.

Denature 1.5 μ l RNA aliquots at 70 C for 2 minutes, then place on ice.

Loading the Gel-Dye Mix

1. Put a new RNA 6000 Nano chip on the chip priming station
2. Pipette 9.0 μ l of gel-dye mix into the well marked G – with circle around it.
3. Make sure the plunger is positioned at 1 ml and then close the chip priming station (you will have to push down hard – till you hear a click).
4. Press the plunger until it is held by the clip.
5. Wait for exactly 30 seconds, then release the clip.
6. Wait for 5 seconds. Slowly pull back plunger to 1 ml position.
7. Open chip priming station and pipette 9.0 ml of gel-dye mix into the wells marked G (no circle).
8. Discard the remaining gel-dye mix.

Loading the Agilent RNA 6000 Nano Marker

1. Pipette 5 μ l of RNA 6000 Nano marker (green) in all 12 sample wells and in the well marked ladder.

Loading the Ladder and Samples

1. Pipette 1 μ l of prepared ladder in well marked ladder.

2. Pipette 1 μ l of sample into each of the 12 sample wells. Pipette 1 μ l of RNA 6000 Nano marker (green) into each unused sample well (final reaction volume of each sample well should be 6 μ l).
3. Put the chip horizontally in the adapter of the IKA vortexer and vortex for 1 minute at 2400 rpm.
4. Run the chip in the Agilent 2100 Bioanalyzer within 5 minutes.
5. Select - Assay, Electrophoresis, RNA, Eukaryotic RNA Nano
6. Select Start
7. Run will take about 25 minutes to complete.
8. After run, click ok, then "Data and Assay"
9. Double click in the sample name field to rename samples, then click the save icon.
10. View results – open a new Word document. Print screen in the 2100 software and paste into the word document. When finished, save the Word document to the desktop (it will remain on the desktop for a few days). Files are permanently stored in the 2100 software, according to date.

Appendix B - Reagents and Supplies

	<u>Company</u>	<u>Catalog Number</u>
<u>RNA Isolation</u>		
TRIzol Reagent	Invitrogen	15596-026
Chloroform	Fisher Scientific	C606-4
Isoamyl Alcohol	Sigma	I-3643
2-propanol (Isopropanol)	Fisher Scientific	A464-4
Ethanol		
Nuclease-Free Water	Ambion	AM9937
<u>DNase Treatment</u>		
TURBO DNA-free	Ambion	AM1907
<u>Reverse Transcription</u>		
SuperScript III	Invitrogen	11752-050
<u>Quantitative PCR (Real-Time)</u>		
Platinum SYBR Green with ROX	Invitrogen	1173-038
<u>Protein Isolation</u>		
M-PER Mammalian Extraction Reagent	Pierce	PI78503
<u>SDS-PAGE</u>		
Ready Gels 12% TRIS-HCL (50 µL/well)	BIO-RAD	161-1156
Precision Plus Standard Dual Color Ladder	BIO-RAD	161-0374
10X Tris/Glycine/SDS Buffer	BIO-RAD	161-0732
Laemmli Sample Buffer	BIO-RAD	161-0737
2-Mercaptoethanol (β-Mercaptoethanol)	Sigma	M-3148
DPBS w/o calcium chloride, w/o magnesium chloride	Gibco	14190-144
Coomassie Brilliant Blue R-250	BIO-RAD	161-0400
<u>Western Blotting</u>		
10X TBS	BIO-RAD	170-6435
Methanol	Fisher Scientific	A452-4
NP-40 Alternative	CALBIOCHEM	492016
Tween-20	BIO-RAD	
Carnation Instant Nonfat Dry Milk		
Super Signal West Femto Maximum Sensitivity Substrate	Pierce	34095
Ready Gel Blotting Sandwiches, Immun-Blot PVDF 7x8.5cm	BIO-RAD	162-0218
R3 Primary Antibody (chicken anti-FSH-R3)		
Secondary Antibody (goat-anti chicken IgY-HRP)	Santa-Cruz	sc-2901
R1 Primary Antibody (chicken anti-FSH-R1)		
R2 Primary Antibody (chicken anti-FSH-R2)		
10x Tris/Glycine Buffer	BIO-RAD	161-0734

	<u>Company</u>	<u>Catalog Number</u>
<u>DNA Isolation</u>		
Dneasy Tissue Kit	Qiagen	69504
<u>DNA gel</u>		
Agarose I	MIDSCI	0710-100G
Ethidium Bromide	Fisher Biotech	BP102-5
<u>Cell Culture</u>		
Dulbecco's Phosphate Buffered Saline 1X w/CaCl ₂ , w/MgCl ₂	Gibco	14040-133
McCoy 5A Medium	Gibco	16600-082
Fetal Bovine Serum	Gibco	16600-044
Penicillin/Streptomycin Stock (5000units/5000 µg/mL)	Gibco	15070-063
Geneticin (G418) (50 mg/mL)	Gibco	10131-035
Trypsin		
EDTA		
DMSO		
Falcon T25 Flasks .2µm vented blue plug seal cap	Becton Dickinson	353109
Costar 6 well cell culture cluster plates 5/bag, 100/case sterile	Corning, Inc.	3506
Pasteur Pipettes	Fisher Scientific	13-678-20C
<u>Other:</u>		
Aloetouch Gloves (small)	Fisher Healthcare	23-667-200A
Diamond Grip Latex Gloves (medium, A&P)	Fisher Healthcare	11-462-67C
Diamond Grip Latex Gloves (large, A&P)	Fisher Healthcare	11-462-67D
Aurelia Protégé Nitrile gloves (medium, A&P)	MIDSCI	93997
Aurelia Protégé Nitrile gloves (large, A&P)	MIDSCI	93998
MAXY clear .6mL Microcentrifuge Tubes	MIDSCI	T-060-C
Fiber Pads Package of 4 (for transfer)	BIO-RAD	170-3933
Rnase-free Tips all sizes (AM12635-AM12665)	Ambion	
Lab Bench Paper 20x250 roll	Fisher Scientific	14-206-65